Chapter 5

TURBOCHARGER AERO-THERMAL PERFORMANCE UNDER REALISTIC FLOW CONDITIONS: PULSATING FLOW AND HEAT TRANSFER CONSIDERATIONS.

Adam Feneley and Apostolos Pesiridis*

Department of Mechanical Engineering, Brunel University London, UK

ABSTRACT

Differences between turbocharger performance on an engine and on a gas stand have been observed throughout decades of turbocharging studies. These differences have been attributed, in part, to various phenomena, the most important of which include heat transfer and pulsating exhaust gas flows that occur on-engine, and that are not commonly captured in experimental turbocharger test gas stands. In early stage design, turbocharger performance maps are regularly used to provide a boundary condition to the engine in gas flow simulations. These maps are typically produced from steady-state gas stand tests, which only cover a limited range of data. Engine performance predictions are therefore determined by air flow and thermodynamic parameters from steady-state compressor maps, which in turn influence the parameters for exhaust gases entering the turbine. If heat transfer effects are not properly accounted for, errors of varying severity will occur in the characterisation of the compressor and the performance prediction of the engine as a consequence. The steady flow conditions of the gas stand tests also determine the turbine map without accounting for the effects of the unsteady pulsating flow that exists under realistic engine conditions, this leads to further errors in the characterisation of the turbine, and subsequently the engine performance prediction. Today, these predictions are being supplemented with CFD analysis, although these simulations are expensive in terms of the hardware and time requirements; efforts to model turbines in this manner are currently outstripping the data available to validate their accuracy. This chapter describes the phenomena associated with heat transfer and pulsating flows in turbomachinery, how they can be modelled, and what their impact is on the turbocharger performance predictions used during early stage engine design.

Keywords: Internal Combustion Engine, Turbocharging, Turbocharger, Heat Transfer, Unsteady and Pulsating Flow

* Brunel University London, Kingston Lane, Uxbridge, UB8 3PH, UK
Email: apostolos.pesiridis@brunel.ac.uk

INTRODUCTION

Emissions regulations around the world have become increasingly strict over recent decades, as governing bodies aim to reduce the emission of harmful gases and particulate matter from internal combustion engines (ICEs). For the automotive industry, which is still dominated by ICE powertrains, turbocharging offers a route to downsize engines, which in turn offers lower fuel consumption and reduced emissions. The key principal of turbocharging is to recover some of the energy lost in the high-temperature and high-speed exhaust gases. A turbine is positioned in the exhaust gas flow path and used to drive a compressor, which is connect by a common shaft; this compressor increases the amount of air injected into the combustion chamber of the engine, therefore increasing available power. By recovering energy in this manner, a larger naturally aspirated (NA) engine can be replaced with a smaller and lighter turbocharged engine that has equal performance but lower fuel consumption.

When designing turbocharged engines, the early-stage design process typically involves performance simulations that are heavily reliant on steady and quasi-steady flow principles. These simulations use steady-flow performance maps as a boundary condition that represents the turbocharger, even though flow in realistic systems is highly unsteady. The performance maps used are typically created from a narrow range of data obtained by gas-stand testing. These maps contain errors stemming from the data extrapolation techniques used, the omission of pulsating flow phenomena and the fact these maps represent the heat transfer phenomena present on a gas stand and not the real-world conditions present in a vehicles engine bay.

OVERVIEW OF UNSTEADY FLOWS IN TURBOCHARGERS

It is widely acknowledged in automotive turbomachinery that highly unsteady flows impact the performance of both turbines and compressors. In the present day, facilities that can emulate the effects of pulsating flows in turbomachinery are scarce. Instead, unsteady CFD investigation is frequently adopted in industry to augment the limited range of steady-flow test data that is available to designers. Both academics [1], [2] and industry [3] are investigating the possibility of incorporating unsteady effects in the turbine into engine simulations. Figure 1 illustrates the fundamental differences between the unsteady flow performance of a turbine, and the equivalent steady flow performance. The hysteresis loop plotted here features anti-clockwise arrows that show the direction of the pulse cycle. This loop corresponds to the open and closed positions of the pulse generator used to create the unsteady flow conditions. [4] Details of how these plots are produced will be given in this chapter under ‘Experimental Analysis of Unsteady Flows in Turbochargers’. Figure 2 is a result of the academic study to date on the effect of pulsating flows on the performance of automotive turbomachinery. The difference between quasi-steady and unsteady efficiency has been plotted for various exhaust gas pulsation frequencies and for a range of speeds. The deviations from the quasi-steady base line seen here are significant, with efficiency prediction errors of between -18% and 12% at 100% of the engine speed range.

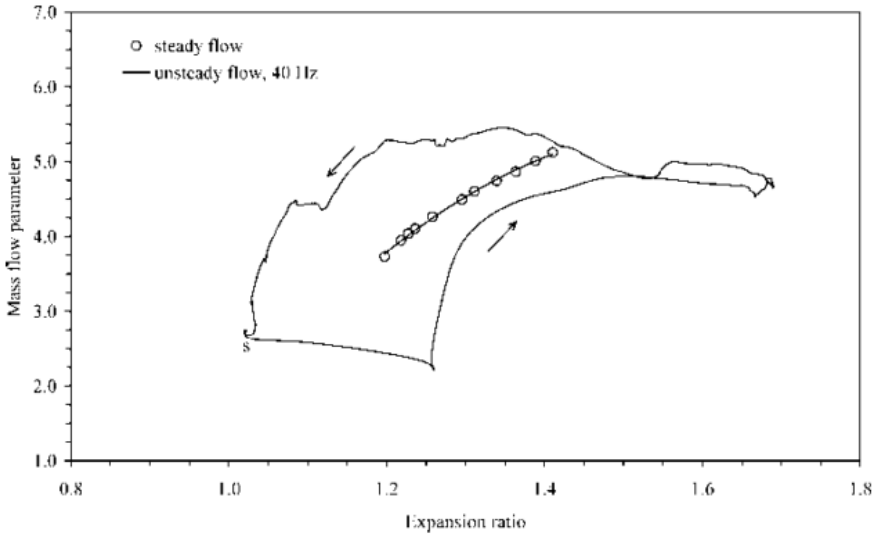

Figure 1 - Illustration of the filling and emptying behavior of a turbine subject to an unsteady flow [4]

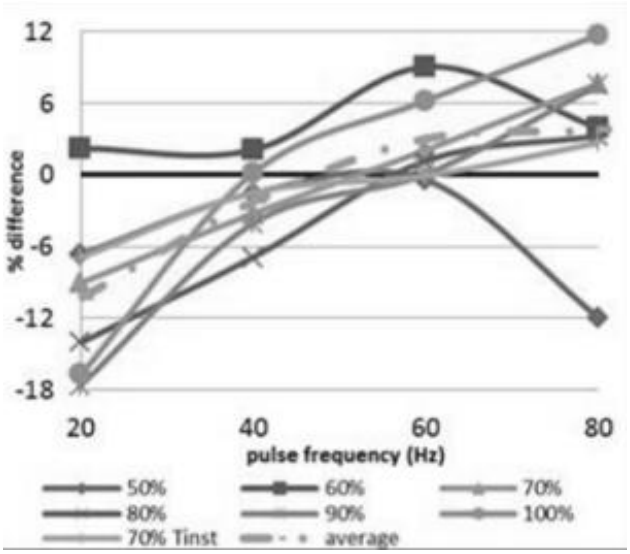

Figure 2 - Percentage deviation of efficiency of turbines subject to unsteady flows [1]

INTRODUCTION TO UNSTEADY FLOWS CONCEPTS FOR TURBOCHARGERS

Non-Dimensional Parameters

The key non-dimensional parameters used when analysing pulsating flow in turbochargers are the mass flow parameter, which is commonly plotted against pressure ratio, and the velocity ratio, which is commonly plotted against efficiency. The mass flow parameter is given by equation 1, and is derived from the relationship between the inlet flow velocity and the Mach number at the inlet:

$$MFP = \frac{\dot{m}\sqrt{T_{tot,in}}}{P_{tot,in}} \quad \text{EQ1}$$

In equation 1 each parameter is an instantaneous, time varying value; this is also the case for every parameter in equations 1-4. The pressure ratio is given by equation 2:

$$PR = \frac{P_{tot,in}}{P_{ex}} \quad \text{EQ2}$$

The velocity ratio is the ratio of the speed of the rotor tip, and the isentropic velocity at the inlet. It can be described by equation 3:

$$\frac{U}{C_{isen}} = \frac{\pi DN}{\sqrt{\left(\left(2\int_{ex,isen}^{in} c_p dT\right) + {C_{in}}^2\right)}} \quad \text{EQ3}$$

The total-to-static efficiency of the turbine is calculated using equation 4:

$$\eta_{t-s} = \frac{\dot{W}_{actual}}{\dot{W}_{t-s,isen}} \quad \text{EQ4}$$

When predicting steady-state performance of a turbocharger turbine, there are two independent non-dimensional parameters that regulate cycle averaged performance; those two parameters are Mach number at the tip, and expansion ratio. When considering unsteady conditions in a turbocharger, assuming that a pulsating inlet flow occurs as a sinusoidal wave, there are four extra non-dimensional parameters that also affect mean turbine performance. This sinusoidal assumption does not adequately represent a true exhaust gas energy wave, it is used here as an initial approximation. With the aforementioned sinusoidal wave assumption, the incoming pressure and temperature waves can be characterized by equations 5 and 6.

$$P(t) = A_P \sin(\omega t) + P_{tot,m} \quad \text{EQ5}$$

$$T_{tot}(t) = A_T \sin(\omega t + \Phi) + T_{tot,m} \quad \text{EQ6}$$

Here, the Greek letter Φ is the phase difference between the pressure and temperature waves. The four new non-dimensional variables are the non-dimensional total amplitude of pressure (A_P/P_{0m}), the non-dimensional total amplitude of temperature (A_T/T_{0m}), the phase difference (Φ), and the Strouhal number (ω/Ω). Here, the Greek letter Ω signifies angular speed of the rotor.

Strouhal Number

The Strouhal number is another key variable found in the analysis of pulsating flows in turbochargers. The Strouhal number may be used as an expression of the relative importance of unsteadiness in oscillating gas flows [5], and can be represented by the ratio of the time taken for a fluid particle to pass through the turbine components (τ_F), and the time scale of the unsteadiness in the pulsating gas flow (τ_p) [6]:

$$St_{F-P} = \frac{\tau_F}{\tau_P} \qquad \text{EQ7}$$

As an approximate guide, if the Strouhal number of the system is close to unity, both quasi-steady and unsteady effects are important, and should be accounted for in any modelling attempt. Values much larger than one signify the domination of unsteady effects; values less than one suggest that quasi-steady effects prevail. Some pulsating flow models represent the rotor differently to the volute section (i.e. with an unsteady volute model, and quasi-steady rotor model), in this case a second Strouhal number may be important [6] and can be expressed by equation 8. Where the time scale for the rotor to spin for one complete revolution (τ_r) is independent of τ_F. When the value of Str_{r-p} is small, steady effects govern performance.

$$St_{r-p} = \frac{\tau_r}{\tau_p} \qquad \text{EQ8}$$

Plotting Unsteady Flow Performance

Finally, when reading studies on unsteady flows in turbomachinery, the most common plots encountered to describe turbine and compressor performance are plots of non-dimensional mass flow parameter vs. pressure ratio and of blade speed ratio vs. total to static efficiency. These are often plotted with a steady-state curve superimposed with an unsteady locus. It is worth noting when observing these graphs that the unsteady loci presented here correspond to a single point on the steady-state curve, and show the behavior of the turbomachine during both filling and emptying processes; authors often do not clearly indicate which point along the steady-state curve that their unsteady locus corresponds to.

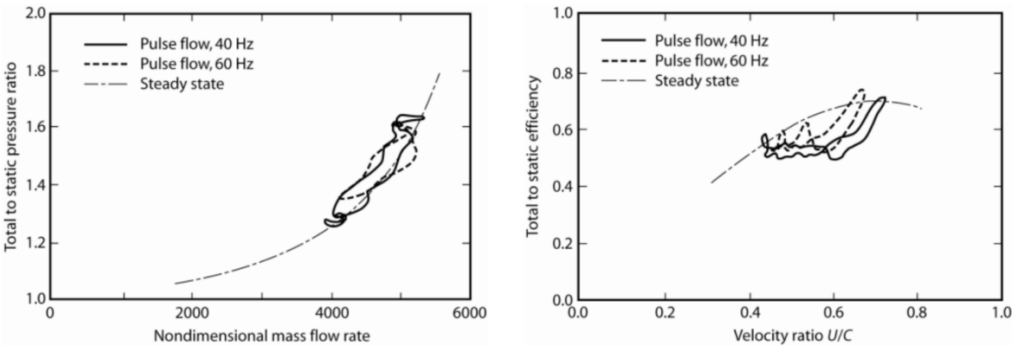

Figure 3 - Turbine performance experimental data under steady state and pulsating conditions [7]

Figure 3 shows an example of this; the 40 Hz and 60 Hz flow lines plotted here correspond to a single point along the steady state curve, which is not identified. Figure 1 is another clear example.

EXPERIMENTAL ANALYSIS OF UNSTEADY FLOWS IN TURBOCHARGERS

The effects of unsteady flows upon the performance of automotive turbocharging have been a major topic of study for several decades. The earliest published experimental studies into pulsating flow in turbocharger turbines were published by Wallace and Blair [8], along with Benson and Scrimshaw [9] in the 1960's. These were followed by Wallace et al. [10], [11], at the end of the decade, and Miyashita et al. [12], Benson [13], and Kosuge et al. [14] up until the end of the 1970's. In the late 1980's and early 1990's, Capobianco et al. [15]–[17] focused on correlating unsteady data with equivalent steady values. However, all of these studies were limited by the instrumentation available at the time, and often only a single parameter was recorded as a time-varying value and other parameters were logged as cycle-averaged values only. It has been noted in a previous review of turbocharger pulsating flows by Baines [18] that these early studies were often contradictory because of these experimental issues. This is because they didn't only show the variance in efficiency under unsteady flow conditions, they also included energy available from the high-pressure ratio of the pulse peaks in exhaust output [18].

The first major studies capable of recording all relevant data as time-varying quantities were conducted at Imperial College London in 1986. The research beginning with the 1986 study by Dale and Watson [7], [19] and continued by Baines et al. [20]–[22], was the first to examine turbine performance data under simulated engine exhaust pulses whilst logging data for all the essential time-varying parameters (except for temperature). This work used a custom-built gas stand with the capability of producing pulsating inlet flows. Figure 3, from Dale [7], shows that there are differences in both flow capacity and aerodynamic efficiency of a turbine tested under steady-state and two different pulsating conditions. Importantly, this study indicated clearly that a turbine does not behave in a quasi-steady fashion under pulsating conditions. However,

the aforementioned continuation by Baines et al. [20], [21] did suggest that the rotor section does operate in a quasi-steady manner under pulsating flow. The similarity of the rotor inlet velocities measured in steady-state flow, and equivalent pulsating flow data (recorded as instantaneous values at equivalent flow conditions, illustrated in Figure 4), indicated that time varying effects must occur in the stator regions, and that they may only occur in these regions.

Later, in the early 1990's, Winterbone et al. [23]–[25] developed a similar unsteady flow test rig that, in addition to recording time-varying flow parameters, could also record values for unsteady turbine efficiency and flow capacity. The key outcome of this study's published data was the non-negligible variation in turbine exit pressure, indicating that the turbine exit boundary conditions should be a key consideration in any modelling setup.

Today, there are still few locations around the world in which pulsating flow phenomena can be investigated through physical testing means. Figure 6 [26] shows one example of a test facility capable of producing unsteady flow test results for turbocharger turbines. The pulse generator is formed of a pair of chopper plates, the profile of which can be designed to replicate the pulse shape of the engine under consideration. The two rotating plates, which can be seen in Figure 8, were designed to separately feed the two limbs of a twin-entry turbine. The plates are driven by a variable speed electric motor, which is used to control the frequency of pulsations. Further details of this test facility can be found in Romagnoli et al [27].

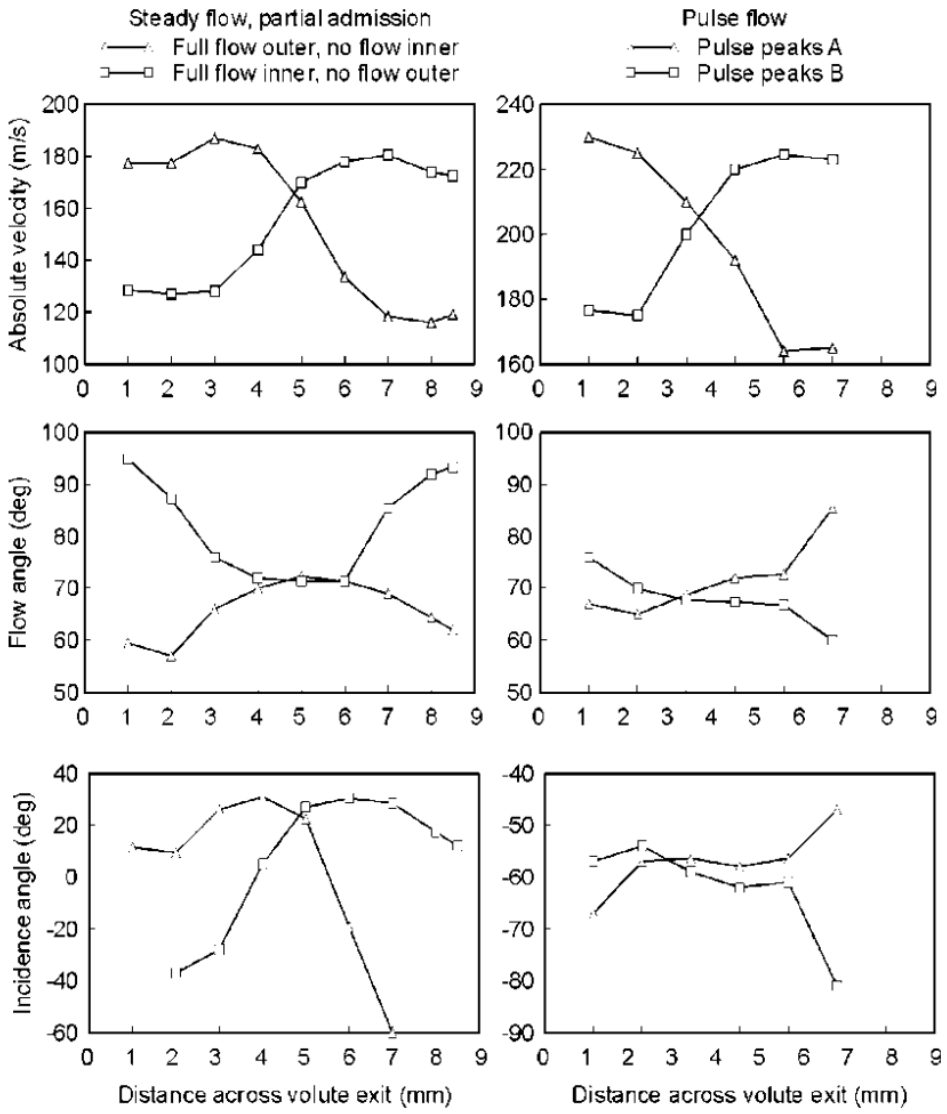

Figure 4 - Steady flow (left) and pulsating flow (right) values of velocity (upper), flow angle (middle) and incidence angle (lower) at the rotor inlet of a twin-entry turbocharger turbine [18]. *Based on data from Yeo and Baines* [20], [21]

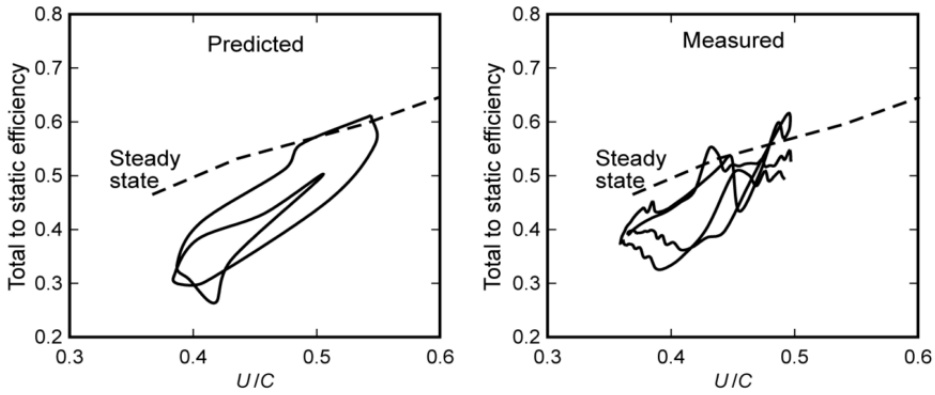

Figure 5 - Comparison with the zero-dimensional model created by Baines et al. [22] *with measured values. The turbine under consideration was a single-entry, nozzleless turbine.*[18]

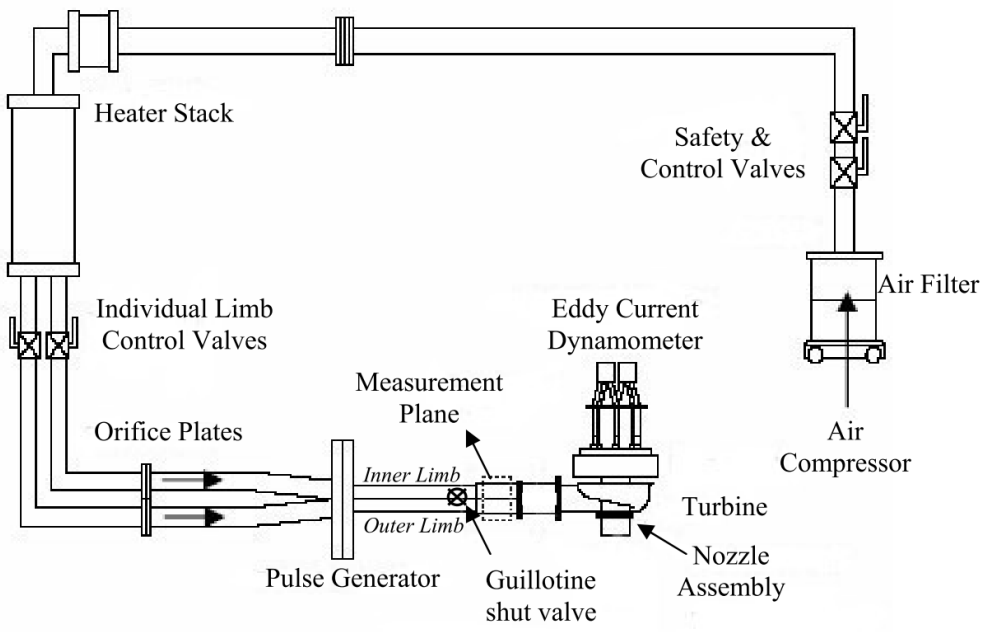

Figure 6 - Schematic of the unsteady flow test facilities available at Imperial College London [26]. A detailed photo of the pulse generator chopper plates can be seen in Figure 8.

The Imperial College facility depicted in Figure 6 is still used today, and has produced a number of more modern experimental studies. In 2002, Karaminis and Martinez-Botas [28] published a study on the unsteady performance of mixed-flow turbines and the comparison of experimental data with steady results. They found that mixed flow turbines achieve peak efficiency at a lower velocity ratio than radial inflow turbines; they also confirmed mixed flow turbines are better able to extract energy from exhaust gases in high pressure operating regions.

In 2005, Szymko et al. [29] used experiment to investigate the behavior of turbocharger turbines subject to unsteady flows. They found the range of velocity ratios present for a given pulse frequency reduces at the pulse frequency increases and that unsteady effects become more prominent at higher frequencies. The authors used modified values of Strouhal number (see the 'Introduction to Pulsating Flow Concepts for Turbochargers' section of this chapter for the basics) to assess when unsteady effects became significant.

In 2007, Hakeem et al. [4] investigated the effect on the geometry of the volute on the unsteady performance of mixed flow turbines. The authors found unsteady test performance parameters showed significant deviation from their steady-state equivalents, implying the steady-state assumption common used for volutes is not applicable; they concluded that volute geometry plays a critical role in the steady and unsteady performance of mixed flow turbocharger turbines. In the same year, Pesiridis and Martinez-Botas [30] used the test facility illustrated in Figure 6 to evaluate the performance of their Active Control Turbocharger (ACT), a turbocharger concept that is designed to actively adapt to the pulsating flow environment by adjusting the inlet area of the throat of the inlet casing to make better use of the exhaust gases' pulsating nature than a typical VGT. Although there were considerable losses shown in the test data, the authors claimed an improvement in power of between 3% and 7% over a regular VGT.

In 2008, Copeland et al. [31] investigated the unsteady performance of a circumferentially-divided, double-entry turbocharger. The authors found that the flow conditions at the turbine wheel were highly dependent on the phase differences between pulses, noting that cycle average efficiency values just average out a complex phenomenon, and that care should be taken when evaluating the effect pulse phasing has on overall performance. In the same year Costall produced his doctoral work [32] on unsteady wave propagation in turbochargers turbines, followed by a paper in 2009 by Costall et al. [33] in which unsteady testing was used to validate a twin-entry turbocharger model, more details of which can be found in the following sub-section of this chapter.

In 2009 [27] and 2010 [26], Romagnoli et al. published a two-part study on unsteady turbine performance for automotive turbochargers. In 2012 [1] Pesiridis et al. used historical experimental tests and a commercial gas-dynamics code to conduct initial investigations into the integration of unsteady effects into standard turbine performance maps. As shown in Figure 2, the authors illustrated significant reductions in turbine efficiency when subject to pulsating flows, the efficiency losses were found to be less significant with increased pulsation frequencies. At the high frequency range, unsteady efficiency was found to be higher than equivalent steady values, as previously indicated by Szymko [34]. In 2014, Yang et al. [35] investigated how the cross sectional geometry of a vaneless turbine housing influences the pulsating flow performance of the turbine.

Additional modern studies have come from the Universidad Politécnica de Valencia (Valencia, Spain), the test facility of which was developed by the CMT group. Here a singular chopper plate is used to generate pulses in the air flow which is powered by a 55kW screw compressor and heated by a series of electrical heaters. Further details can be found in the paper by Serrano et al [36]. Figure 8 shows the difference between the pulse generator chopper plates used by Imperial College London and Valencia, with the Imperial facility accommodating twin entry turbines, and the Valencia facility optimized for testing single entry turbines.

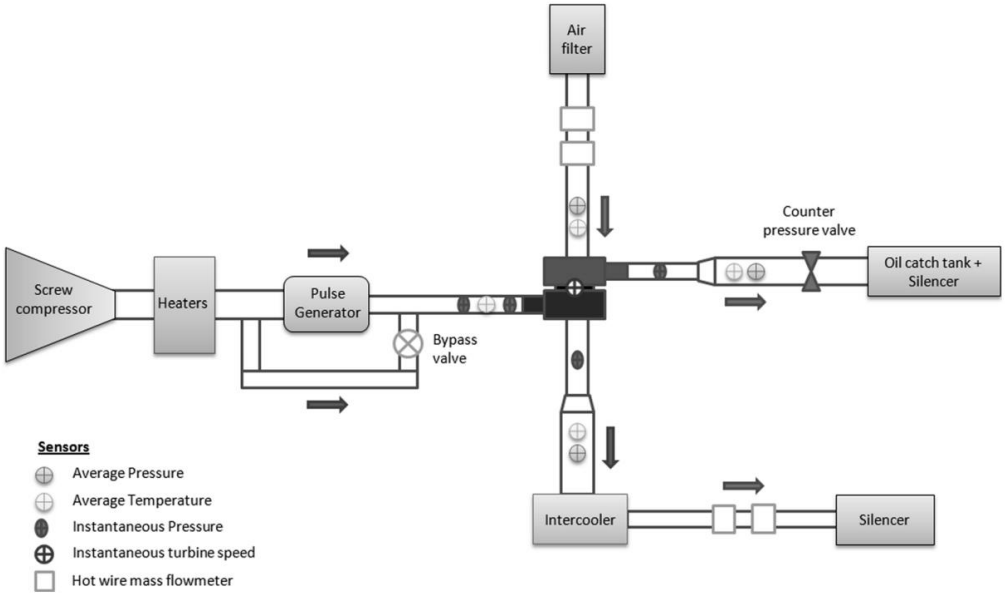

Figure 7 - Schematic of the test facility at the Universidad Politécnica de Valencia, designed by the CMT group [36]

The research group based in Valencia have published papers detailing test plans for the comprehensive characterization of automotive turbochargers [37]. In a 2012 study [36] a team at Valencia used this test facility to collect a wider range of efficiency data than is typical in industry in order discuss the importance of using wide data ranges when predicting unsteady performance. This testing program also investigated the effect of the frequency and amplitude on the efficiency of a VGT (Variable Geometry Turbocharger [38]), and the authors developed a database of their results. [36] The authors found the efficiency of the turbine is least affected by pulsations and amplitudes close to the value of blade speed ratio measured at maximum efficiency, it was also concluded that larger pulse amplitudes reduce the cycle average turbine efficiency in the VGT.

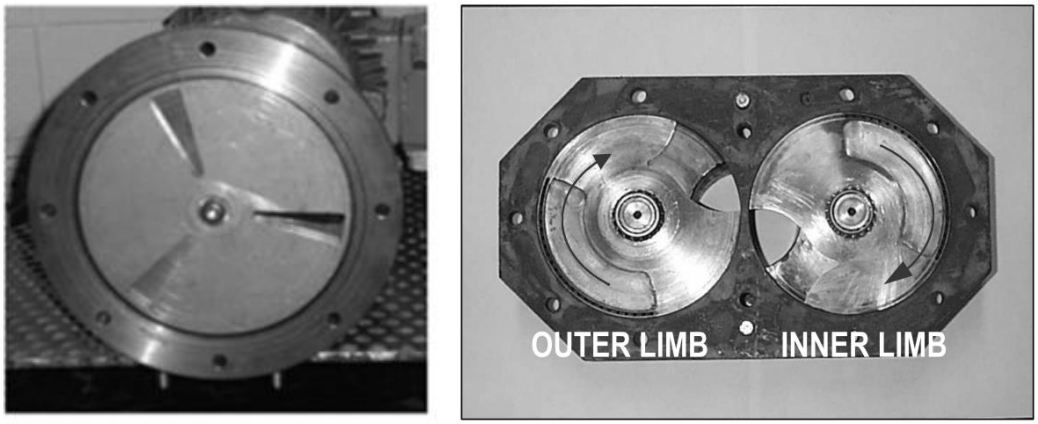

Figure 8 - Difference between the single chopper plate system used by Valencia (left) and the dual chopper plate system used at Imperial College London (right). The Imperial facility allows for two separated airflow streams.[26], [36]

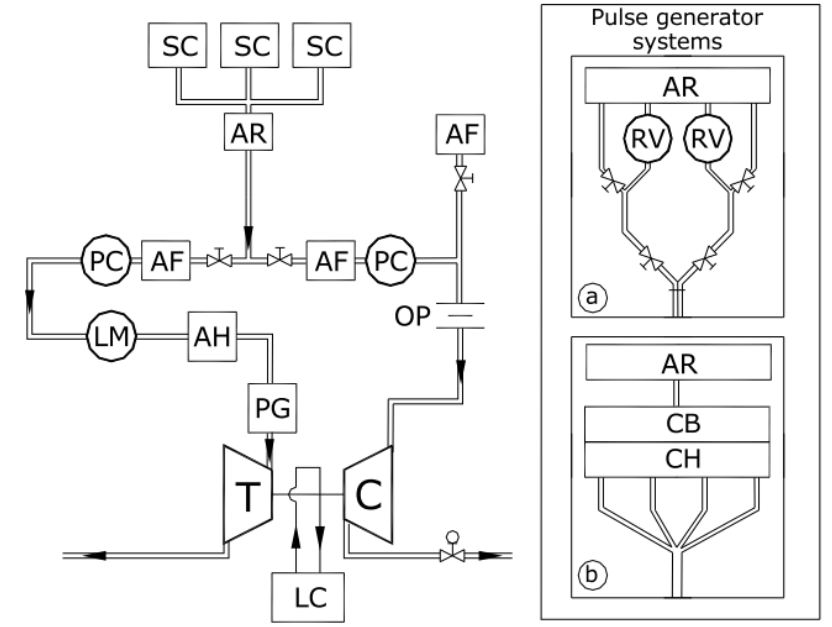

AF Air Filter	LM Laminar Flow Meter
AH Air Heater	PC Pressure Control
AR Air Reservoir	PG Pulse Generator
C Compressor	OP Orifice Plate
CB Cylinder Block	RV Rotating Valve
CH VVA Cylinder Head	SC Screw Compressor
LC Lubricating Circuit	T Turbine

Figure 9- Schematic of the unsteady flow test facilities found at the University of Genoa, Italy [39]

Further modern experimental work has been undertaken at the Università di Genova (Genoa, Italy) [39], [40] using the test facility illustrated in Figure 9, further details can be found in papers by Capobianco and Marelli [41], [42]. Three electrically driven screw compressors supply air, and the compressor is used as a dynamometer, allowing for investigations to take place over an extended data range.

In 2007, Capobianco and Marelli [42] conducted unsteady flow testing on the rig illustrated in Figure 9 in order to investigate the effect of waste-gate control on turbine performance. In 2010 [39] and 2011 [40], the same authors conducted an experimental study on the same facility that aimed to investigate the unsteady flow behavior in an turbocharger turbine whilst taking into account the opening of the waste-gate valve opening. They found that waste-gate opening increased the amplitudes of oscillations for every parameter they considered (pressure, temperature and mass flow), increasing the overall system unsteadiness and affecting turbine unsteady flow performance. Unsteady flow performance was found to deviate most substantially when the waste-gate valve was open. In 2011 [43] and 2014 [44], Bozza et al. used data from this same testing setup to verify unsteady turbine modelling efforts, these will be covered in more detail in the following sub-section. A 2011 study by Capobianco and Marelli [45] performed unsteady testing that highlighted the difficulties encountered measuring instantaneous values.

MODELLING OF TURBOCHARGER UNSTEADY FLOWS

The 1994 study of Baines et al. [22] adopted a zero-dimensional modelling approach when building on the pioneering experimental study of Dale and Watson [19]. Zero dimensional methods have since been surpassed, but this early modelling attempt uncovered some major findings and achieved good agreement with test data. The model introduced a ‘residence time’ to gas flow entering a volute (representing the volute); this is often described as the filling and emptying method for modelling unsteady flows. The rotor was treated as quasi-steady in this case, and modelled using orthodox one-dimensional steady-state techniques. Figure 5 shows the results achieved with this model compared to the experimental data; this was the first study to record all key parameters as time-varying quantities, and is described in the previous sub-chapter.

One-Dimensional Unsteady Flow Models

The next step forward from this was in applying one-dimensional modelling techniques, which had previously been used to model fluid flow in pipes and manifolds, to turbomachinery [46]–[48]. Since this methodology can be used for the turbine, connecting pipes and the manifolds, it is possible to create a model of the entire system with a consistent method. This would also provide numerical consistency, providing that these techniques adequately described the performance of turbines. When using 1D modelling and faced with pulse frequencies typically found in an IC engine, quasi-steady behaviour of the turbine stage cannot be presumed [8], [9], [19], [20], [29]. However, to compensate, a duct may be placed before

the quasi-steady turbine boundary condition to characterize the volume, allowing filling-and-emptying to occur [22], [33].

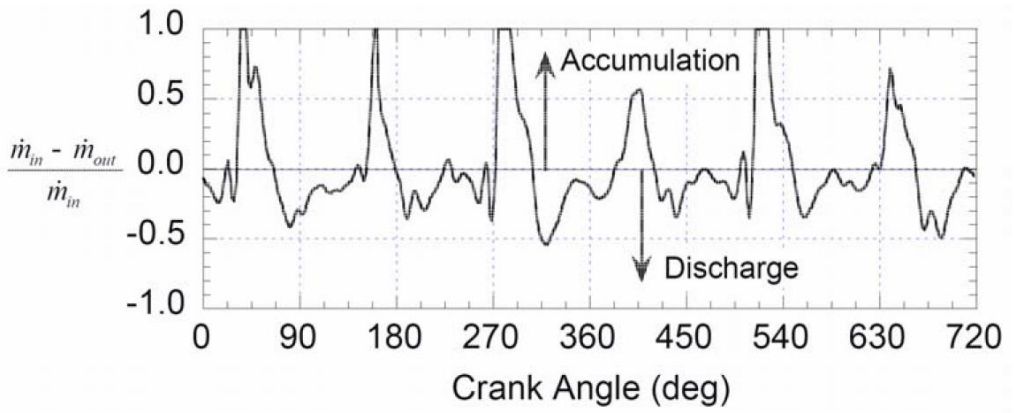

Figure 10 - Illustration of the mass accumulation and discharge (A.K.A filling and emptying behaviour) that occurs in a turbocharger turbine subject to unsteady flow. Plotted across 720 degrees of crank angle, or one engine cycle. [49]

The study by Winterbone et al. [24], [25] was built open by Chen et al. [50] who built a one-dimensional model of a radial inflow turbines without any nozzle components (vaneless), with a quasi-steady rotor model. The volute in this early model was represented by a tapered pipe. The one-dimensional equations were solved with a first-order accurate method. This model was later developed by Abidat et al. [51] who instead treated the volute as a curved pipe with an inlet area equal to the tongue section of the volute, and an exit equal to the mean area and radius of the volute; the area of the pipe was assumed to vary linearly, and the solver was second order accurate. The authors concluded that their study showed an improved agreement with experimental data compared to the work of Chen et al [23], [50]. The unsteady flow model predicted loops which were observed experimentally, while the curve obtained with the quasi-steady assumption coincided with the constant speed curve.

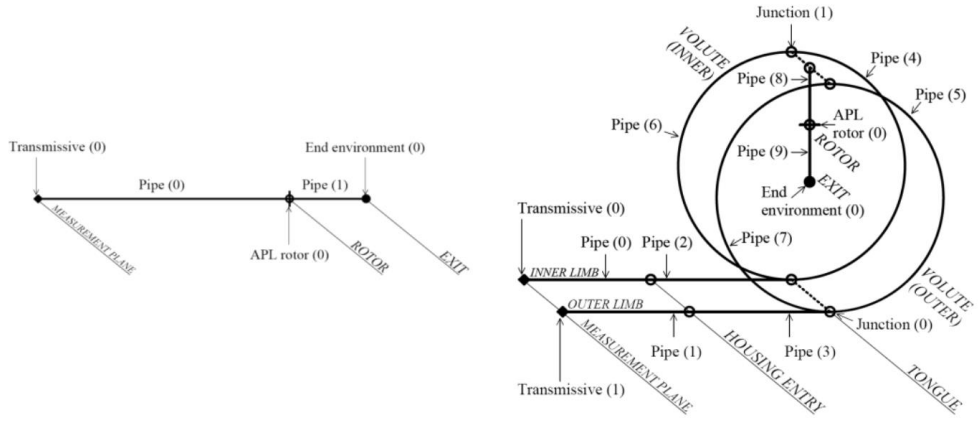

Figure 11 - Schematic of modelling techniques used by Costall et al.[33], [52]

Costall et al. [33], [52] of Imperial College London, advanced this 1D methodology further, with studies on single and twin-entry turbine modelling. Figure 11 shows simple representations for the modelling of single entry (on the left) and twin-entry (on the right) turbines. The aim of the single-entry model was to create the most basic model conceivable that could resolve both filling-and-emptying and wave action effects; the pipe was proportioned to serve as the total volume of the volute under consideration. [18] The twin-entry model permits rotor losses as well as, at the junctions, stator losses. The authors concluded that the single-entry model was successful at predicting mass flow and power at 60Hz, but it's evident from these graphs that the twin-entry model wasn't as effective. It was specified that the twin entry model is necessary when it comes to simulating pulses that are produced out of phase, the different pulses need to be applied concurrently to the domain [33]. The authors proposed that the reason the twin-entry model under projected mass flow was the poor choice of loss coefficients, since the rotor boundary governs the total flow capacity.

Complex One-Dimensional Unsteady Flow Models

The next step along from these simple one-dimensional models is a model that can account for unsteady flows within the rotor itself, and provide a more rational representation of the flow and geometry. Complex one-dimensional models have been developed to remove to quasi-steady rotor and model the complete turbine, including the rotor, using unsteady flow principles. Following the study by Ehrlich [53], [54] on the nature of unsteady turbine inlet flow, more complex one-dimensional models have been developed by Hu and Lawless [49], [55], [56] and King [57]. In these models the solution is found along the mean streamline, with each nozzle passage treated as a separate element with a radial and axial component. This means adopting a sliding plane approach, where the stator is solved in an absolute frame and the rotor in a relative frame; the model can therefore predict time accurate flow fields for individual rotor passages. However, this type of model does have various drawbacks, for example a twin-entry turbine is not modelled with any mixing between the two streams. Furthermore, for model setup of nozzleless turbines, a constant rotor inlet angle is required as an initial assumption. [18] The biggest problem however, is how the model deals with losses. In the aforementioned studies by Hu and King, these forces were estimated by comparing turbine efficiency and steady-state mass flow with their isentropic counterparts and it was assumed that all loses occurred in the rotor. For a more realistic model test data is needed for each section of the turbine, but this is often not available.

More recently, Chen and Winterbone [6] published a complex one dimensional model that allows circumferential feeding of the rotor from the volute. In this case, the volute was represented more rationally by using a large set of geometric input data to represent the entirety of the volute, the length and area of each flow passage segment. The result is a 'curved slot model' of the turbine volute, which in this case was used to predict the performance of a vaneless radial turbine; this can be seen in Figure 12. Similar to previous models, a key drawback here is the simplistic manner with which losses are handled. In addition, between the mean line of the volute passage and the entry to the turbine the flow is assumed to have a constant pressure and density, which is not a rational representation of real conditions. Plots provided in this study showed the model can capture unsteady flow characteristics such as hysteresis loops similar to those observed by Dale and Watson [19], they also showed rational

changes in flow angle fluctuations at different azimuth angle positions as shown in Figure 14. The model predicted notable fluctuations in flow angle close the tongue section of the volute (Figure 13 (a)) and damping of flow angle fluctuations at earlier azimuth angle locations. A further model was produced by Feneley et al. [58] building upon the work of Chen, including an unsteady rotor model and giving significant detail on the modelling process, this model also predicted similar flow angle fluctuation close to the tongue, and damping effects in the rest of the volute, although was not verified with test data.

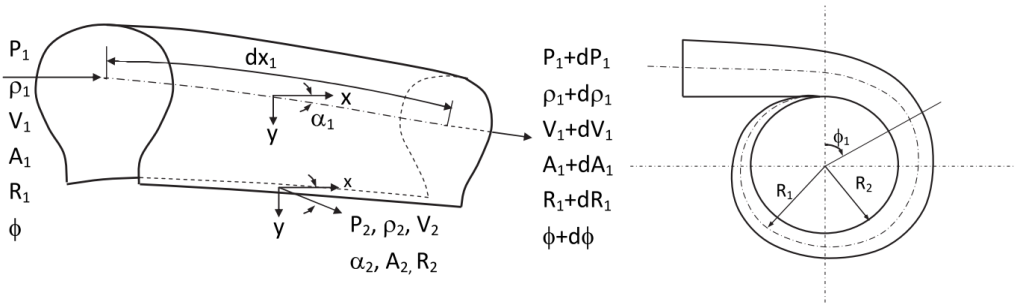

Figure 12 - Schematic of the modelling approach taken by Chen and Winterbone [6]

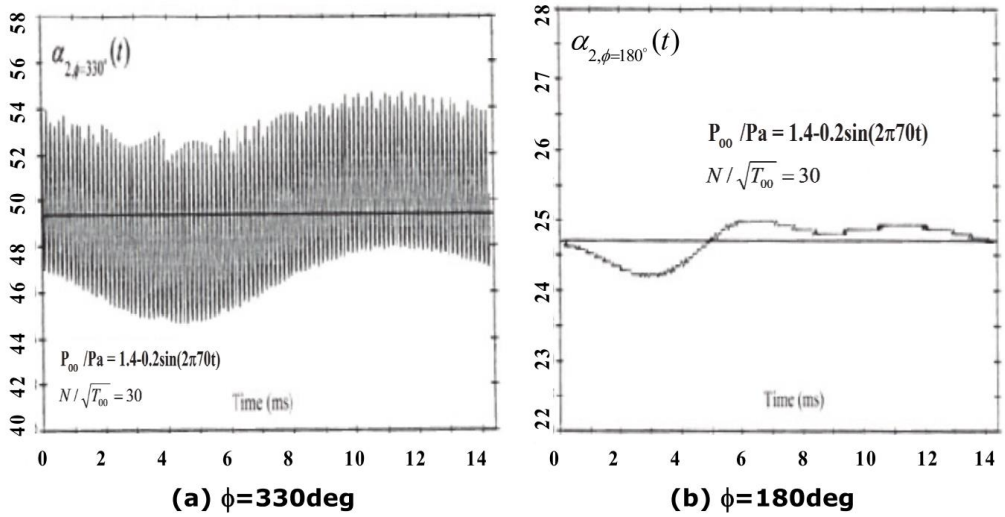

Figure 13 - Flow angle variation predicted by the model of Chen and Winterbone with variation of azimuth angle

Multi-Dimensional Unsteady Flow Models

One step above these complex one-dimensional models are three-dimensional flow models. The majority of pulsating flow studies for turbochargers focus on evaluating turbine performance rather than analysing 3D flow phenomena. Three-dimensional (3D) modelling essentially involves modelling the time-varying Navier-Stokes equations for the turbine. 3D methods are capable of investigating aerodynamic features of pulsating turbine flow. Using the frozen rotor method, (with multiple reference frames) this was attempted in the earliest publication on the subject by Lam et al [59]. The report presented no comparison with test data,

but results were consistent with previous observations [18]. Another method, presented in the work of Palfreyman and Martinez-Botas [60], used a nozzleless turbine in which the rotor was explicitly rotated during the calculation using a sliding mesh. This study was the first three-dimensional model to be validated using test data. However, multi-dimensional methods are highly computationally expensive; the Palfreyman and Martinez-Botas study produced over 100Gb of data with "computing times certainly outside the time scales associated with today's design environment" according to the authors [60].

In studies from KTH in Stockholm, Hellström et al. [61]–[63] reported a the use of LES (Large-Eddy Simulations) to model pulsating flow in a turbocharger. Hellström argued that the large-scale eddies, which are solved by LES, are important in turbine pulse flow. Standard LES practice was used whereby the energy cascade allows energy to transfer between length scales, when the smallest scales are handled by a model, and larger eddies are solved using Navier-Stokes. A variety of inlet conditions were investigated: with and without turbulence, and with different combinations of swirling flow and vorticity. The result was a variation of around 20% difference between time-averaged power values across all inlet boundary conditions. Figure 14 shows a velocity field produced by Hellström and Fuchs [61] using an LES simulation, it is worth noting that although these show detailed results, they are not validated against test data. Complex experimental methods may be required to validate LES models; such as the use of laser-based PIV (Particle Image Velocimetry) and a transparent turbine housing to produce an instantaneous velocity field, which could then be compared with a plot such as that shown in Figure 15. There are examples of using laser techniques have been undertaken in turbochargers in the past, such as when Karamanis and Martinez-Botas [64] used laser doppler velocimetry to visualize internal turbocharger flows, but these have not been used to verify 3D simulations to date.

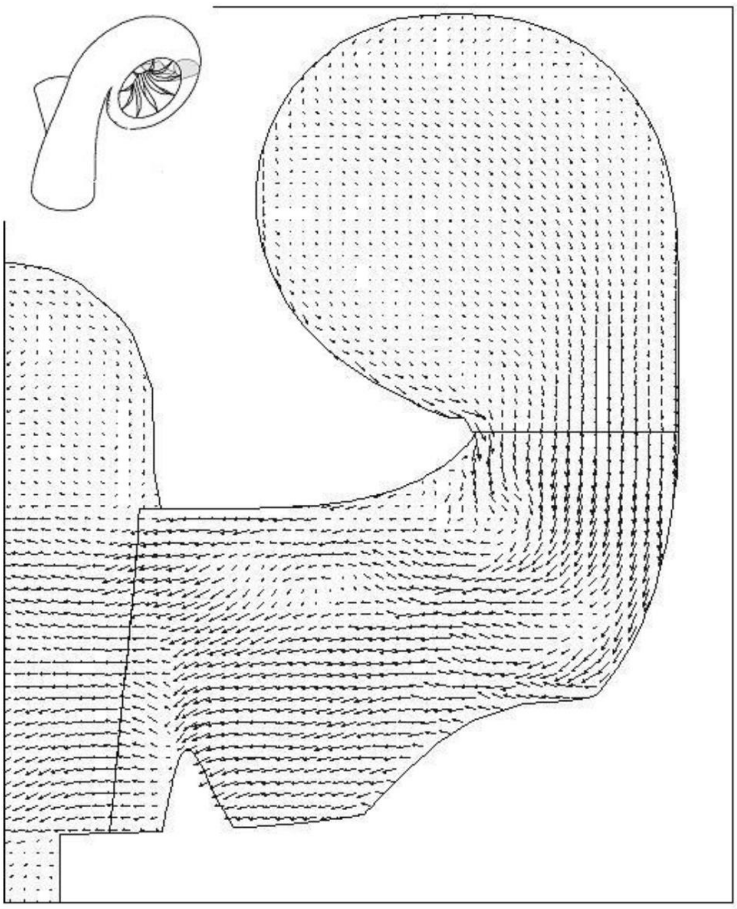

Figure 14 - Example velocity distribution plot produced by the LES simulation of Hellstrom and Fuchs [61] *The cross section is shown in the top left. The snapshot here shows an instance of high mass flow; the arrow length is defined by the magnitude of velocity, the orientation of each arrow defines the flow direction*

HEAT TRANSFER EFFECTS ON TURBOCHARGER PEFORMANCE

Overview

Turbochargers are subject to a complex and significant heat transfer environment when located on an internal combustion engine. Notably, heat flows from the turbine side to the relatively colder compressor side; this has a significant impact on the peformance of the compressor, particularly at low mass flow rates and rotational speeds. Figure 15 shows the effects of turbine exhaust gas temperature on the efficiency of the turbocharger compressor. In the same manner as the turbine, steady-flow gas stand measurements are typically extrapolated to create performance maps for compressors in industry. These compressor maps do not take into account the effects of heat transfer in realistic engine conditions, instead they represent a

degree of heat transfer specific to the gas stand conditions; gas stand flow temperatures are typically condisderably lower than real-world operating conditions.

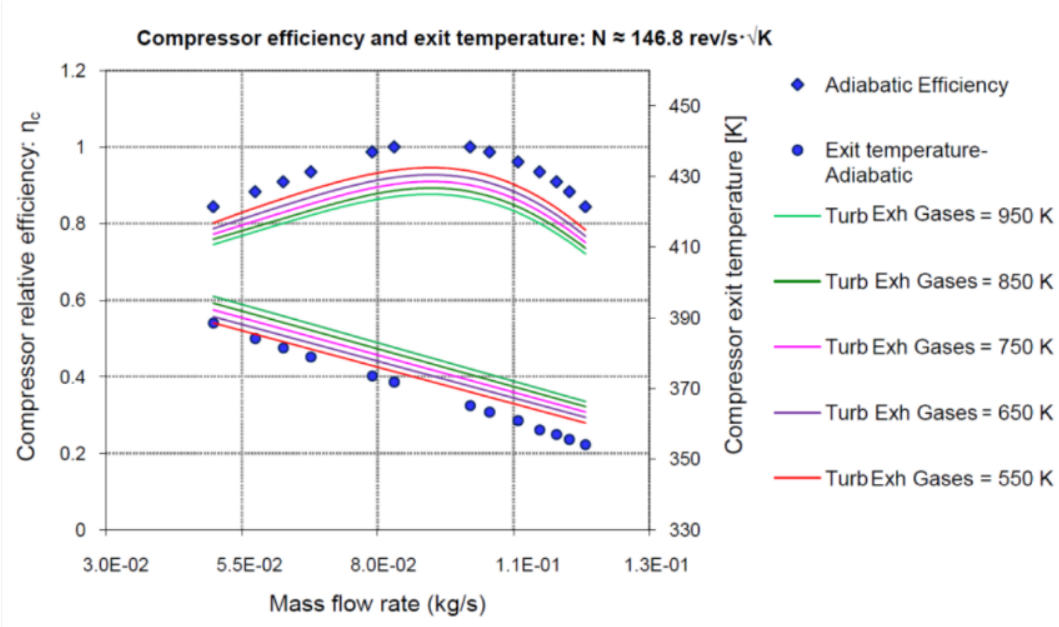

Figure 15 - Compressor relative efficiency vs. Mass Flow rate for a range of turbine exhaust gas temperatures

The failure to account for an accurate heat transfer picture at this early-stage leads to errors in the performance prediction of turbochargers and engines in commercial software. Inspecting Figure 15, it can be observed that higher exhaust gas temperatures created larger deviations in compressor performance when compared with the adiabatic assumption commonly used by simulation codes. When predicting compressor power, errors can reach up to 48% if heat transfer is not included in calculations [65].

INTRODUCTION TO TURBOCHARGER HEAT TRANSFER CONCEPTS

Automotive turbochargers operating under engine conditions are subject to significant heat transfers, but these have rarely been accounted for in the industry when modelling performance. Various studies have suggested that efficiency findings vary significantly when these effects are taken into account. The publications that have dealt with heat transfer in the past invariably involve the analysis of adiabatic and diabatic processes. The turbocharger is typically assumed to be adiabatic if the temperature measured at the turbine inlet is less than 100 degrees Celsius [66]. Models of energy transfer have been developed and will be discussed; since conduction and radiation processes can be calculated with existing material properties, the main challenge lies with modelling forced and free convection. Figure 16 summarises the key modes of external and internal heat transfer relevant to turbochargers.

The ideal reference for a turbocharger is a diabatic, non-ideal process [67]; this represents the process in on-engine conditions or on a hot flow gas stand, which can then be compared with an adiabatic, non-ideal process. This ideal scenario, although rarely used in industry due to its practical difficulty and limitations, can be simulated on a gas stand by minimizing heat transfers. Insulation reduces external heat transfer, and controlling the temperatures of the air, oil and exhaust gas helps to minimize internal energy flows. Industrial models often rely on diabatic gas stand efficiency [67], in which total enthalpy change is calculated as the algebraic sum of work and heat transfers. Since adiabatic testing is technically challenging and limited to a certain operating range, common practice uses diabatic methods with no correction for on-engine values; despite heat transfer differing from the gas stand conditions.

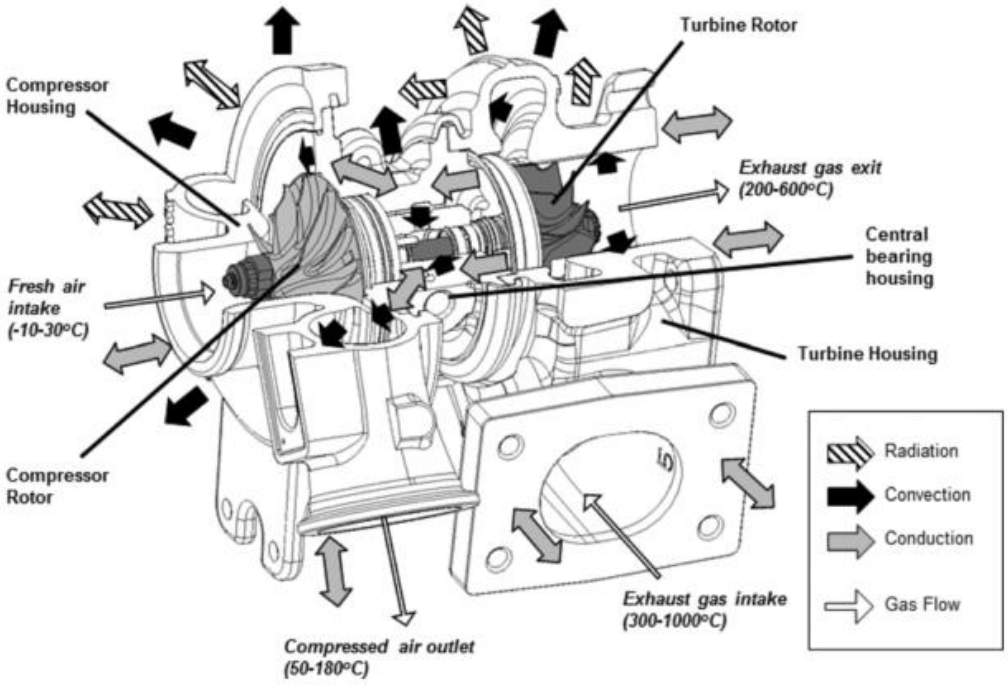

Figure 16 – Heat transfer processes in a turbocharger [68]

Adiabatic testing is practically useful for finding an accurate measure of work transfer, the total enthalpy change is equal to the shaft work transfer and can be found my measuring total temperatures at the inlet and exit. The main objectives of adiabatic testing could also be achieved my measuring shaft power directly; using a device such as a dynamometer.

When conducting the most common [67] test used in industry (diabatic), the process is considered to be adiabatic, plus heat transfer. This method often assumes that heat transfer occurs after the work transfer. This assumption seems reasonable when considering the compressor side of a turbocharger, but less-so in the turbine section. Considering the compressor, this assumes that work transfer occurs mostly in the impeller, beginning at the inlet; heat transfer then occurs in the volute and diffuser sections. Given the greater surface area

for heat transfer to occur in the volute this seems a reasonable assumption in the compressor. In the turbine this assumption means most heat transfer occurs before the turbine rotor. However, total inlet enthalpy occurs at the inlet of the rotor, and is affected by heat transfer. Specific work transfer and total inlet enthalpy of the turbine are related, such that their quotient is equal to a constant [67].

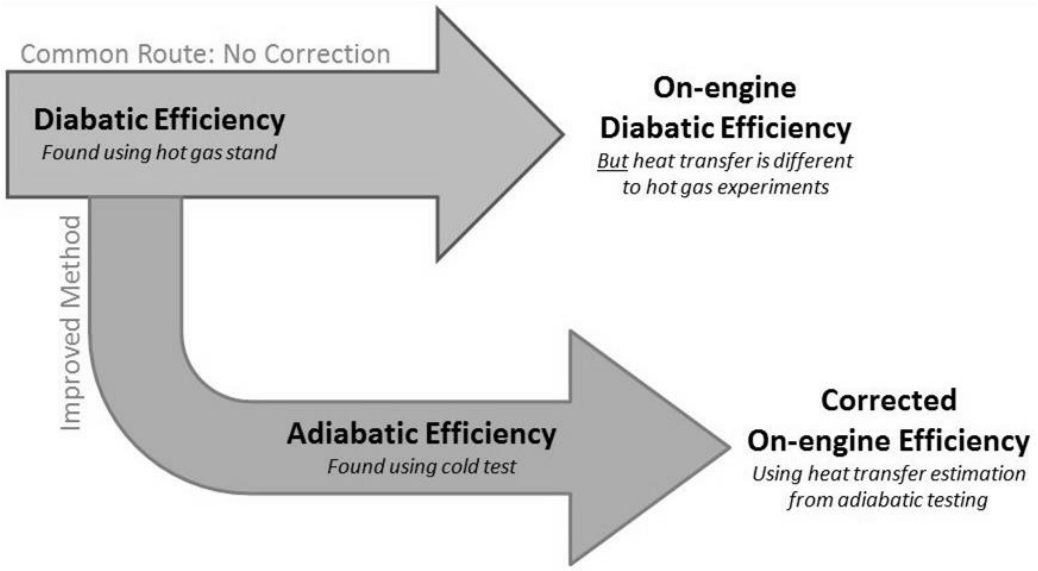

Figure 17 - Methods of applying tested efficiency to on-engine conditions

The conventional diabatic test can be improved upon if an estimate of heat transfer can be obtained, this can then be used to correct the efficiency to obtain an adiabatic efficiency (Figure 17). Since adiabatic efficiency is only subject to internal gas dynamics inside the turbocharger, it can apply to both on-engine operation and gas stand tests. Adiabatic efficiency can therefore be readapted for on-engine heat transfer.

External Heat Transfer Processes

Heat transfer processes in an automotive turbocharger (Figure 16) can be grouped into internal and external processes. The external processes involve heat transfer to the surroundings; such as air, fixings and other components. These external processes consist of radiation, convection and conduction. In on-engine operation it is often the case that many of the adjacent components will be of a very similar temperature to the turbocharger itself. However, given the flexibility and density of engine bay layouts, most studies model the conduction to adjoining parts by using a conduction coefficient. The following equation describes external heat transfer for a turbocharger given the above assumption also applies to convection and radiation which can be calculated with an ambient 'sink' temperature [67]:

$$Q_{ext} = \theta_e A_e (T_e - T_a) + \varepsilon\sigma\left({T_e}^4 - {T_a}^4\right) + \kappa A_c (T_e - T_a)/x \qquad \text{EQ9}$$

$$Q_{ext} = \quad Q_{conv} \quad + \quad Q_{cond} \quad + \quad Q_{rad}$$

The temperature of the fluid inside the turbocharger (T_f), as shown in Figure 19, drives internal and external heat transfer, it can be related to the external surface temperature (T_e) with equation 10:

$$\frac{Q_{ext}}{A} = \theta_i(T_f - T_i) = \frac{\kappa}{t}(T_i - T_e)$$

$$(T_f - T_i) = \frac{Q_{ext}}{A\theta_i}$$

$$(T_i - T_e) = \frac{Q_{ext}}{A\left(\frac{\kappa}{t}\right)}$$

$$\therefore (T_f - T_e) = \frac{Q_{ext}}{A}\left(\frac{1}{\theta_i} + \frac{t}{\kappa}\right) \quad \text{EQ10}$$

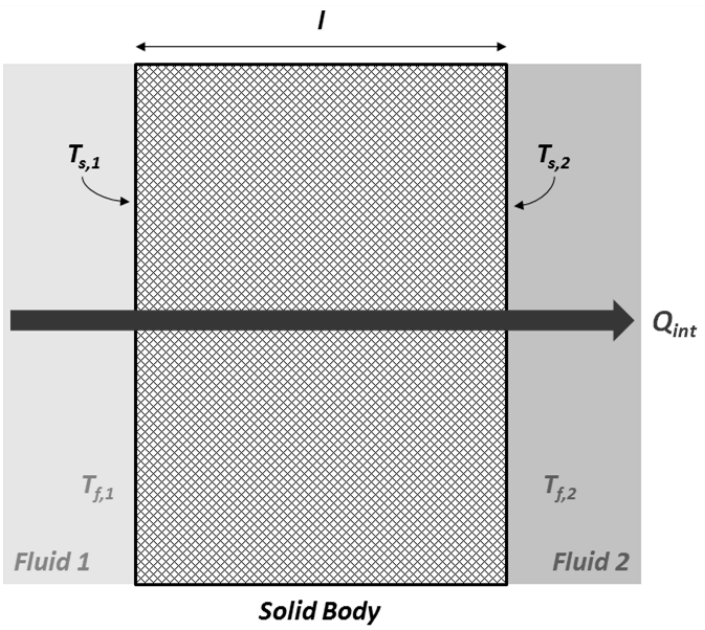

Figure 18 - Internal heat transfer between two fluids in a turbocharger

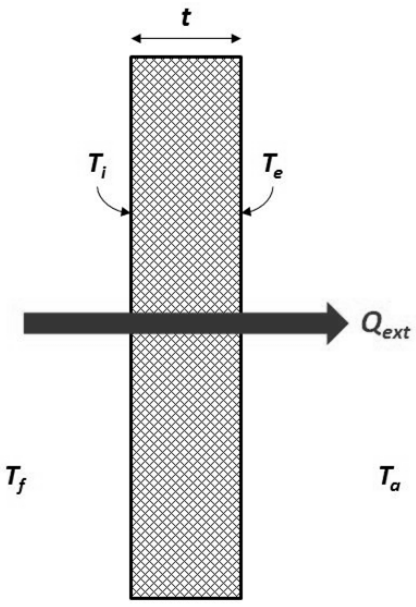

Figure 19 - 1D consideration of heat transfer through the housing wall

For the purpose of modelling heat transfer, these equations (EQ9 and EQ10) can be solved to find the two unknowns (T_e and Q_{ext}) providing all other coefficients are known.

Internal Heat Transfer Processes

Internal heat transfer concerns the convection and conduction of heat between components of the turbocharger. Although there are radiation effects, they are small in comparison to conduction and convection and are usually assumed to be negligible. Considering the one-dimensional heat transfer between two internal turbocharger fluids (Figure 18), across a solid

body of length '*l*', where the temperature of the surfaces in contact with fluid 1 and 2 are $T_{s,1}$ and $T_{s,2}$ respectively; the internal heat transfer can be described with the following:

$$\frac{Q_{int}}{A} = \theta_{f,1}(T_{f,1} - T_{s,1}) = \frac{\kappa}{l}(T_{s,1} - T_{s,2}) = \theta_{f,2}(T_{s,2} - T_{f,2})$$

$$(T_{f,1} - T_{f,2}) = \frac{Q_{int}}{A}\left(\frac{1}{\theta_{f,1}} + \frac{l}{\kappa} + \frac{1}{\theta_{f,2}}\right) \quad \text{EQ11}$$

If the fluid temperatures are known, along with the various heat transfer parameters, equation 11 can be used to model the internal heat transfer [67]. In addition to the theory outlined in this section, modelling of heat transfer processes that can describe physical conditions depend upon the knowledge of: fluid and ambient temperatures, emissivity of the housing components, thermal conductivity of all relevant components, and convective heat transfer coefficients for all interfaces.

Forced convection is a common mechanism in which fluid motion is generated by an external source; a useful ratio is known as the Archimedes number (Ar). At values greater than 1, natural convection is dominant, and lower than 1 is where forced convection is dominant. This is given by:

$$Ar = \frac{Gr}{Re^2} \quad \text{EQ12}$$

Where Re is Reynolds number and Gr is the Grashof number:

$$Re = \frac{\rho C L}{\mu} \quad \text{EQ13}$$

$$Gr = \frac{\chi g \rho^2 L^3 \Theta}{\mu^2} \quad \text{EQ14}$$

In free convection Reynolds number tends to zero and buoyancy forces (Grashof number describes the ratio of buoyancy to viscous force) dominate. The general expression for forced convection is given as:

$$Nu = a\, Re^b Pr^{\,c} \quad \text{EQ15}$$

Where *Nu* is the Nusselt number, a, b and c are constants and *Pr* is the Prandtl number; these are expressed as:

$$\mathrm{Pr} = \frac{C_p \mu}{\kappa} \quad \text{EQ16}$$

$$Nu = \frac{\theta L}{\kappa} \quad \text{EQ17}$$

The length scale L in equations 13, 14 and 17 is the stream-wise distance. When investigating instances where ventilation is negligible, equation 17 can be replaced with [67]:

$$Nu = d\ Gr^{e} Pr^{f} \quad \text{EQ18}$$

Where d, e and f are constants. This equation can be of use to describe the external heat transfer from the surface of a turbocharger when ventilation is negligible.

When looking to quantify turbocharger performance, total to static efficiency (η_{ts}) and the mass flow rate parameter (MFP) are commonly used, and their expressions are shown by equation 4 and equation 1 respectively. These equations are for adiabatic processes, and as such their use cannot be justified for the calculation of diabatic reversible flows, since it is not isentropic [69]–[71]. Prior studies have used the assumption that heat transferred during this process is negligible [26], [72], [73] and so only included heat transferred before and after the process.

For the purpose of analysing h/S diagrams for the compressor and turbine, a new system of subscripts is needed that is separate from the numerical subscripts used in the rest of the report. For the following discussions, this numerical system of turbocharger locations applies:

1	Compressor inlet	3	Turbine inlet
1*	Impeller inlet	3*	Rotor inlet
2	Compressor outlet	4	Turbine outlet
2*	Impeller outlet	4*	Rotor outlet

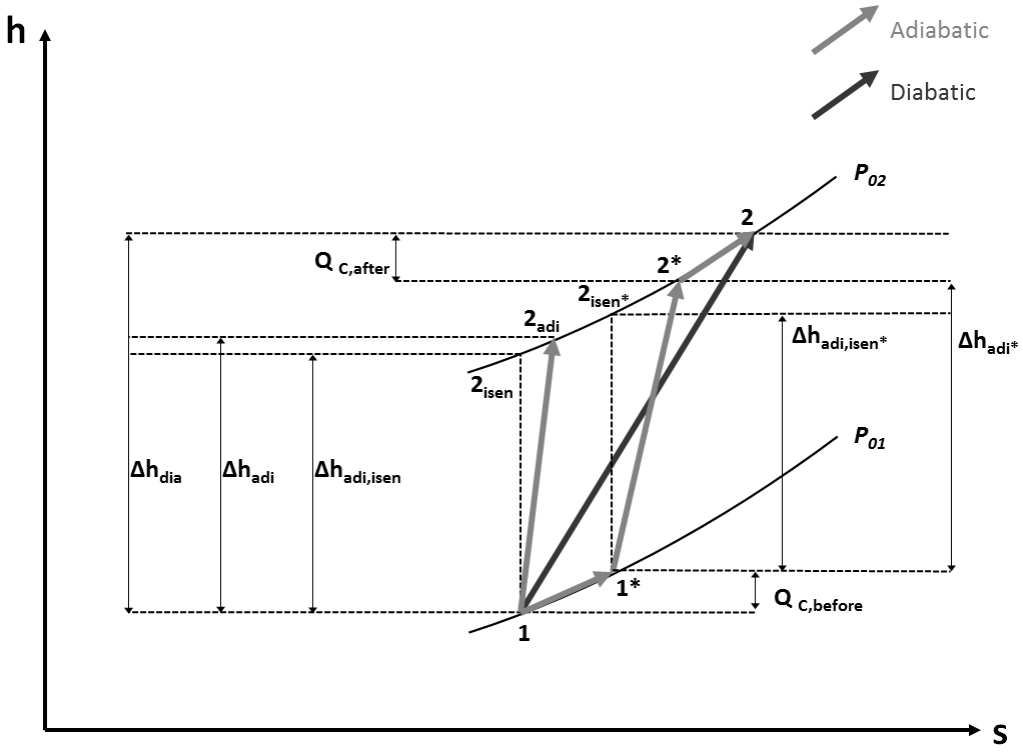

Figure 20 – h-S diagram for a compressor

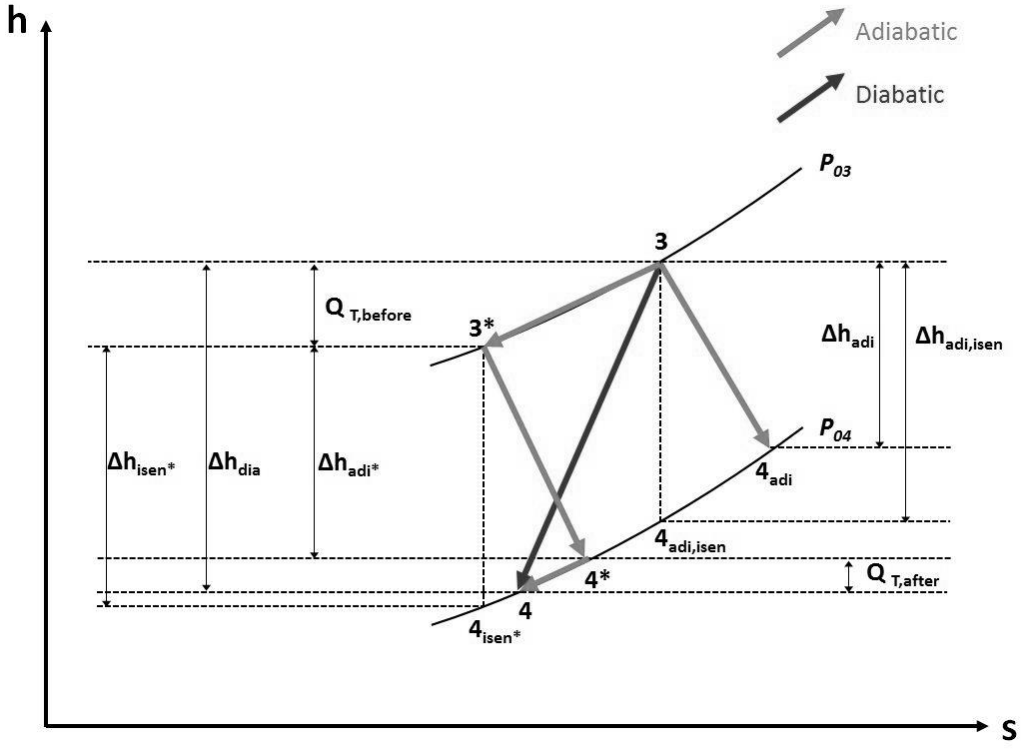

Figure 21 – h-S diagram for a turbine

Figure 20 shows the h-S diagram for a turbocharger compressor, illustrating adiabatic and diabatic processes; heat transfer before and after the process are labelled. Process 1-2_{adi} represents the adiabatic compression, and process 1→2 shows diabatic compression. An isentropic process from point 1 would simply proceed vertically up to point 2_{isen}; point 2 is the end point for a diabatic compression process, which would have higher temperature and therefore enthalpy [72]. The diabatic process flows from 1→1*→2*→2, but the expansion process 1*→2* is assumed to be adiabatic. Two separate heat transfer processes can then be defined between 1→1* and 2*→2, as before and after the compression process ($Q_{C,before}$ and $Q_{C,after}$). The diabatic and adiabatic efficiency of the turbine can be calculated with the following expressions [72]:

$$\eta_{C,dia} = \frac{\Delta h_{adi,isen}}{\Delta h_{dia}} = \frac{T_{2,isen} - T_1}{T_2 - T_1} \quad \text{EQ19}$$

$$\eta_{C,adi} = \frac{\Delta h_{adi,isen}}{\Delta h_{adi}} = \frac{T_{2,isen} - T_1}{T_{2,adi} - T_1} \quad \text{EQ20}$$

Similarly, the turbine h-S diagram (Figure 21) illustrates the adiabatic expansion (3→4_{adi}) and the diabatic expansion (3→3*→4*→4). In this case the expansion process in the diabatic case (3*→4*) is assumed to be adiabatic and the heat transfer is again defined in two parts; before and after the expansion process. As with the expansion of the compressor, the turbine efficiencies can be calculated from the h-S diagram by using the following relations:

$$\eta_{T,dia} = \frac{\Delta h_{dia}}{\Delta h_{adi,isen}} = \frac{T_3 - T_4}{T_3 - T_{4,isen}} \quad \text{EQ21}$$

$$\eta_{T,adi} = \frac{\Delta h_{adi}}{\Delta h_{adi,isen}} = \frac{T_3 - T_{4,adi}}{T_3 - T_{4,isen}} \quad \text{EQ22}$$

In a 2006 study [74] which investigated the prominence of mass flow and speed in the compressor, Shaaban and Seume successfully quantified the relationship between adiabatic and diabatic efficiency in turbochargers:

$$\frac{\eta_{C,dia}}{\eta_{C,adi}} = \left(1 + K_{C,before}\xi_C\right)^{-1}\left(1 + \frac{\xi_C}{\gamma_{air} - 1}\frac{1}{{M_{p,2}}^2}\frac{1}{\epsilon\left(\frac{1-\varsigma_2}{\tan\beta_{2*}}\right)}\right)^{-1} \quad \text{EQ23}$$

$$M_{p,2} = \frac{u}{\sqrt{\gamma R T_{1,tot}}} \quad \text{EQ24}$$

$$\varsigma_2 = \frac{C_{2*,mer}}{u} \quad \text{EQ25}$$

Analysing equation 23, it can be seen that the peripheral Mach number (M_p), as a squared value, is the key parameter in determining compressor performance. Notably, as flow coefficient (ς) increases, the right-most term decreases; creating a larger deviation between efficiencies. This all implies that the efficiency ratio tends to unity as peripheral Mach number increases. A compressor with low values of heat number and high peripheral Mach numbers can be assumed to be working under adiabatic conditions [72].

EXPERIMENTAL STUDIES OF TURBOCHARGER HEAT TRANSFER

The earliest experimental investigations into heat transfer effects in turbochargers were conducted in the 1980's by Rautenberg et al. [75], [76] and Malobabic and Rautenberg [77]. These studies were focused upon comparing hot and cold test results. Cold tests are characterised by spinning the turbine with air that is fairly close to ambient temperatures; typically the aim here is to recreate adiabatic conditions so the heat transfers phenomena can be separated from other losses that occur in the turbocharger. The pulsating-flow test facilities at Imperial College London, for example, can conduct these cold tests on just the turbine mounted to the flow apparatus; facilities elsewhere exist where these tests can be performed on the entire turbocharger (including the compressor).

Hot tests are more commonly used, particularly in industry (see Figure 23). These hot gas stand tests generate diabatic maps, which account for a specific quantity of heat transfer (which corresponds to the gas stand, and *not* realistic engine conditions) and other losses associated with the turbocharger. The most common mode of testing, used by industry to create performance maps, involves exposing the turbocharger to ambient conditions, whereby external heat fluxes can be measured. However, it is also possible to totally insulate the outer surfaces of the turbocharger in order to measure internal heat fluxes (see Figure 22).

Figure 22 - A fully insulated turbocharger turbine, with attached thermocouples [78]

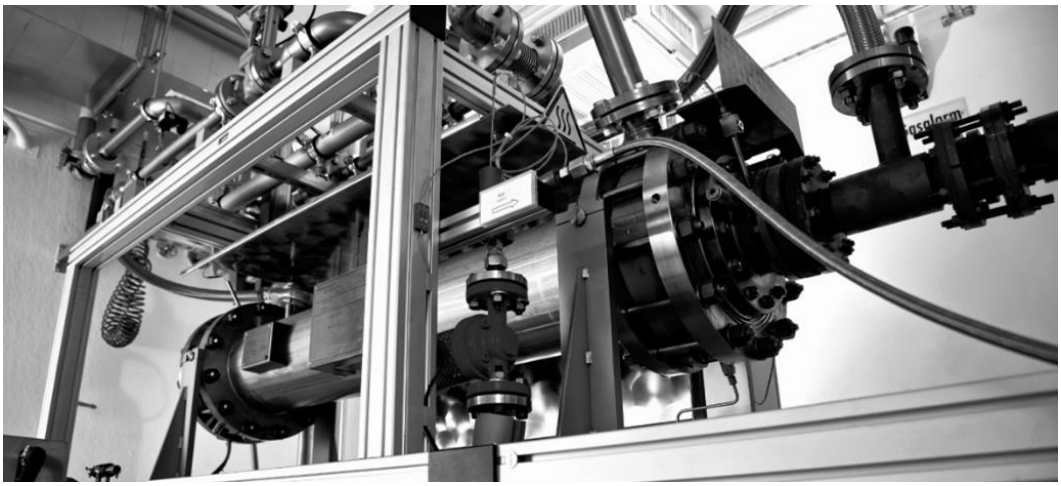

Figure 23 - Turbocharger hot gas stand, such as those used in industry. This example was produced by Kratzer Automation, a market leader in turbocharger test benches [79]

For analysis and the production of maps, parameters recorded in both hot and cold tests include temperature and pressure at the inlet and exit of the turbine and compressor, mass flow rate of each working fluid, and rotational speed of the common shaft connecting the compressor and turbine wheels. Table 1, derived from records collected by Romagnoli et al. [80], shows the typical equipment used for each parameter, and references of example studies which have adopted the relevant experimental methods:

Table 1- Experimental instrumentation used to measure various parameters required for the production of turbocharger maps for the purpose of analysing heat transfer

Parameter	Relevant Instrumentation	Example Experimental Studies
Gas mass flow	Venturimeter	Shaaban & Seume [81], Rautenberg et al. [75]
	Hot wire	Burke et al. [82], Serrano et al. [83], Romagnoli & Martinez-Botas [84]
	Hot film sensor	Burke [85], Burke et al. [86]
Oil mass flow	Coriolis flow meter	Payri et al. [87], Verstraete & Bowkett [88], Serrano et al. [89]
Temperature	K-type thermocouple	Serrano et al. [89], [90]
Oil temperature	Platinum resistance thermometer	Sirakov & Casey [69], Payri et al. [87]
Pressure	Piezoelectric/piezo-resistive sensors	Burke et al. [82], [91], Serrano et al. [83], [92], Cormerais et al. [93], Burke [85]
Rotational speed	Eddy current sensor	Shaaban & Seume [81], Burke et al. [91]
	Inductive sensor	Chesse et al. [65], Cormerais et al. [66]

Thermal imaging can also be a useful experimental tool, Figure 24 shows the result of one such experimental test by Tanda et al. [94]. The left hand image and overlaid chart shows

minimal external heat variation during quasi-adiabatic testing, where temperatures are marginally higher in the bearing housing, on the right however diabatic testing shows far greater variation in external surface temperatures along the axial direction. When using thermal imaging in this manner, it is advisable to use a specialist coating in order to increase the thermal emissivity of the surfaces, and to ensure the thermal emissivity values are equal. The temperature gradients displayed in the right hand image are in part the result of the differing thermal conductivity values of the turbine, bearing and compressor housings.

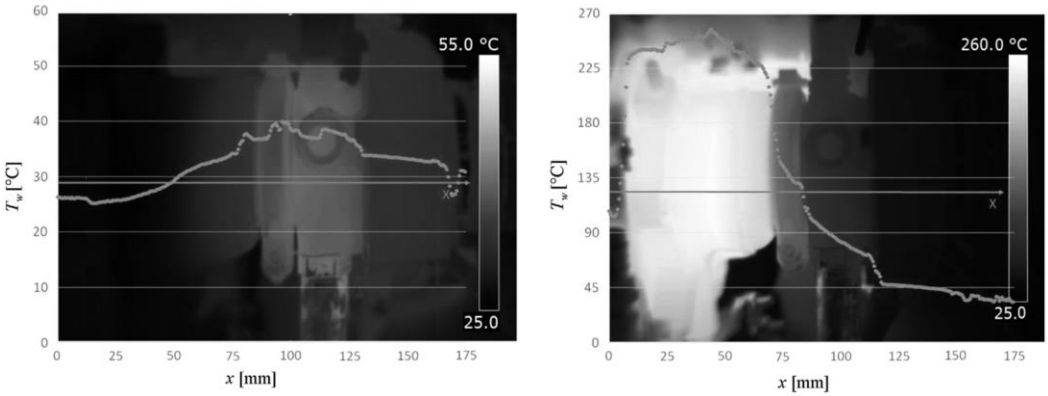

Figure 24- Thermal imaging test results of a turbocharger at quasi-adiabatic conditions (left) and diabatic conditions (right).[94]

In 2002, Jung et al. [95] performed experiments that were amidst the first to determine the impact of heat transfer on the sections of turbocharger performance maps in regions that are typically neglected in industry. The authors didn't succeed in correlating their findings with a function, but results did show that heat transfer had a significant impact in low speed environments, and that they can be considered negligible in high speed flow conditions [65], [96]. Researchers experimentally investigating compressor maps [65], [66] noted that as turbine inlet temperature increased constant speed lines of the compressor maps remain constant. Authors noted that this adds evidence to support the modelling assumption that heat transfer takes place after the turbine wheel [80]. Various authors [65], [95], [96] showed that plots of pressure ratio against corrected mass flow for the compressor is unchanged, and therefore immune from effects caused by heat transfer. However, changes in compressor outlet temperature do significantly alter efficiency plots and low speed conditions, leading to non-negligible drops in performance. A 2017 study [94] explained that at high pressure ratios, heat transfer effects are mitigated by the additional absorption power of the compressor. In order to adapt maps, correction models can be adopted to alter conventional maps; such models have been developed for both compressors [97] and turbines [98].

Turbine inlet temperature (TIT) is an important factor in turbocharger performance and its significance has been noted and investigated by various studies. TIT has a much higher impact on the temperature of the housing than external heat transfer, and turbine heat transfer is primarily a function of TIT [67]. For example, inner and outer wall temperature variations can reach up to 50 kelvin as TIT increases, which can negatively affect turbine efficiency [84], [99]. Baines et al. [67] found that reducing TIT by 100 degrees Celsius caused maximum heat flow to be reversed in the turbine housing. The maximum temperature of the turbine housing has a

linear relationship with TIT, compressor housing's also share a linear relationship when subject to high mass flows [87].

On the compressor side, where operating conditions are also a key driver of heat transfer, the oil temperature was found to have a larger impact than TIT by Sirakov and Casey [69]. Shaaban and Seume [81] discovered that 30% of the heat transfer away from the turbine was in the oil. Serrano et al. [100] wrote that compressor outlet temperature decreases when oil temperatures rise above that of the compressed air. Also, as the oil temperature increases, it's viscosity decreases, causing Reynold's number to rise. Romagnoli and Martinez-Botas stated this reduction in viscosity allows even more heat to be absorbed by the oil, improving its coolant effect [84].

Insulated turbines, such as that pictured in Figure 22, offer a chance to study internal heat fluxes without heat loss to ambient air. It is estimated that when a turbocharger is not insulated, that 50% of heat loss from the turbine is to the ambient air [67], this loss from the turbine can account for up to half of the enthalpy drop in the turbine [87]. When not insulated, the compressor absorbs more radiant heat from the turbine than it loses through convection to the environment. Areas with larger contact areas and high temperatures are responsible for the bulk of heat loss to ambient.

Experimental investigations have revealed some key findings on the quantification of efficiencies. Early work by Rautenberg et al. [76], published in 1984, observed a notable 3.3 point difference between adiabatic and diabatic efficiencies when running at 70,000 rpm; this difference was found to increase as the physical distance between turbine and compressor housings was reduced. At 60,000 rpm, Shaaban and Seume [81] recorded a 55% difference between turbine power under diabatic and adiabatic conditions. As a result, volumetric efficiency was found to decrease between 3% and 4% near the compressor surge condition; this effect of reduced turbine power and increased compressor power may lead to turbo lag [81].

Burke et al. [86] provided some key comparison when producing their own convective correlations in 2015, the resulting table and graph are shown in Table 2 and Figure 25 respectively. Nusselt number was previously given in its general form in equations 15 and 18; the variation shown in the relationship between Nusselt number and Reynolds number in Figure 25 is due to changes in fluid density [80]. It's clear to observe that different studies have concluded with diverse solutions, this is because of the dissimilar way that each study defined characteristic length (see column 4 of table 2). Baines et al. [67], Cormerais [101], Reyes-

Belmonte [102] and Burke et al. themselves, conducted experimental testing to arrive at their correlations; Romagnoli and Martinez-Botas's 2012 study [103] was a theoretical work.

Table 2- Nusselt number correlations for turbocharger turbines, from Burke et al.[80], [86]

Authors	Source	Correlation	Characteristic length	Constants		
				a	b	c
Baines et al. (2010)	Gas stand	$Nu = aRe^b Pr^c$	L_{volute}	0.032	0.7	0.43
Cormerais (2007)			D_{inlet}	0.14	0.75	1/3
Reyes-Belmonte (2013)	Gas stand	$Nu = aRe^b Pr^{\frac{1}{3}} \left(\frac{\mu_{bulk}}{\mu_{skin}}\right)^{0.14} F$ where $F = 1 + 0.9756 \left(\frac{\frac{D_{inlet}}{\eta_{max}}}{\frac{(L_{volute})^2}{4D_{inlet}}} \right)^{0.76}$	$\frac{(L_{volute})^2}{4D_{inlet}}$	1.07 5.34 0.101	0.57 0.48 0.84	1/3 1/3 1/3
Romagnoli and Martinez-Botas (2012)	Theory	$Nu = aRe^b Pr^c$	$\frac{D_{inlet}}{2}$	0.046	0.8	0.4

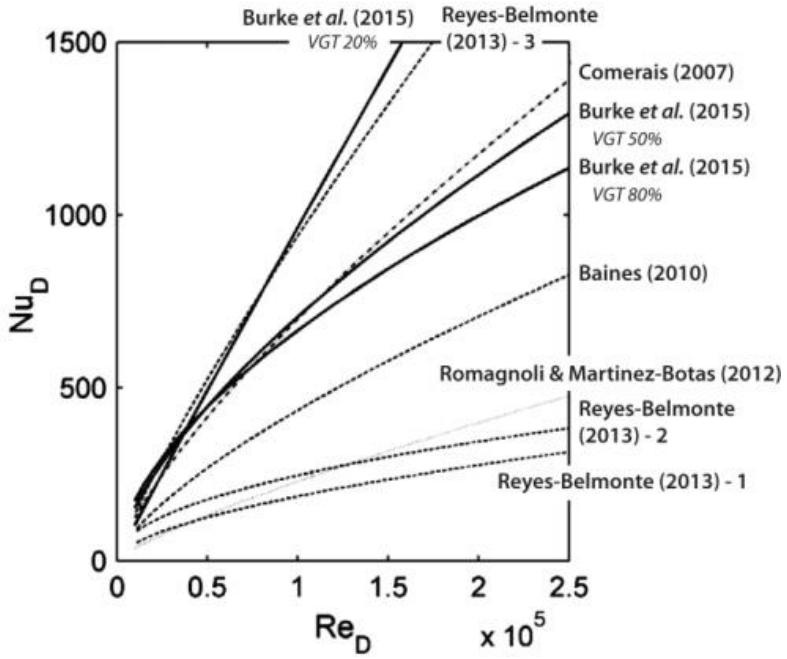

Figure 25 - Comparison of fitted convection correlations, from Burke et al.[80], [86]

HEAT TRANSFER MODELLING FOR TURBOCHARGERS

One-Dimensional Heat Transfer Modelling

A common approach to modelling heat transfer within turbochargers is to adopt a one-dimensional lumped-capacitance model. This is a simplified system that represents each element of the system as a metal node, each element is connected by a virtual circuit and the properties of their interaction is defined. The resulting system is analogous to an electrical

capacitance and resistance model [80]. The energy storage of each of the nodes (turbine, compressor and bearing housing) is modelled by the capacitor attached to each. Each turbocharger component is assumed to be a simplified body with a known geometry; linear temperature distribution dominates, while radial distribution of temperature is neglected. Figure 26 shows an example one-dimensional lumped capacitance model by Serrano et al. [83] Commonly, Newton's law of cooling is used to solve for conduction, the Sieder-Tate correlation is used to solve convection, and, when appropriate, Boltzman's law can be used for radiation. Models that use the lumped capacitance method come with the assumption that heat transfer and work occur independently, with the heat flow taking place before expansion and after the compression; the expansion and compression processes themselves are often assumed to be adiabatic. The variables required to solve such a model are usually obtained from experimental testing. Testing, or 3D modelling should usually be required to validate any assumptions [104] made in one-dimensional models.

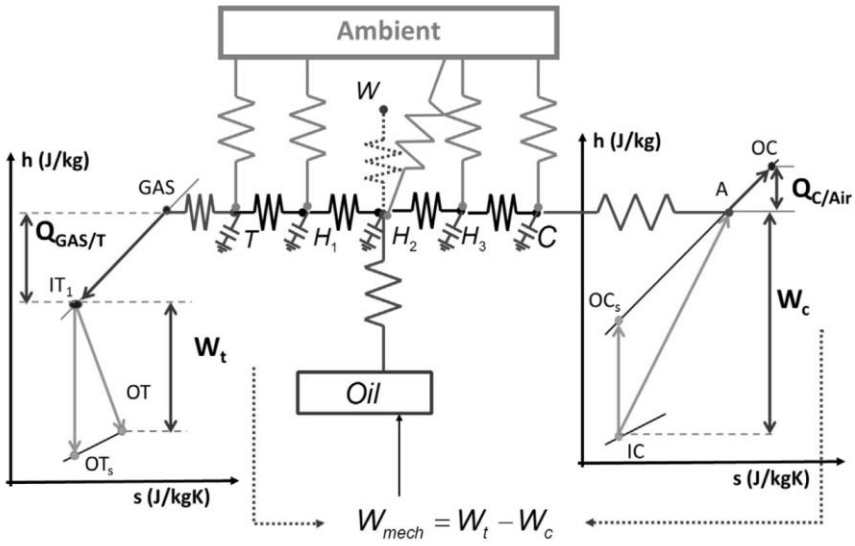

Figure 26 - Schematic of a one-dimensional lumped capacitance model adopted by Serrano et al.[83]

In modern commercial one-dimensional gas dynamics software, used to simulate the performance of powertrain components, turbochargers are a boundary condition and their performance is dictated primarily by the turbine and compressor maps input by the user. Much of the research undertaken in this area has been investigating accurate prediction of the turbine outlet temperature and the compressor outlet temperature, as these will have a significant impact on the engine-turbocharger matching process. A summary of one-dimensional modelling attempts is provided in Table 3, from Romagnoli et al. [80], representing a collection of the one-dimensional modelling attempts by various research groups, giving details of their equations, assumptions and methodology.

Table 3- Summary of 1-D heat transfer modelling to date, from Romagnoli et al.[80] *(Page 1 of 3)*

No.	Reference	Model type	Focus	Analysis type	Assumptions	Equations	Prediction and recommendation
1.	Olmeda et al.	1-D lumped model	Prediction of turbocharger outlet properties and heat flux	Steady	1. Radial temperature distribution is negligible 2. No external heat transfer 3. No radiation 4. Turbine side – Heat transfer Occurs only before expansion 5. Compressor side –Heat Transfer occurs only after compression	Convection: Sieder – Tate: $(h.A)_{l/i}\ k.a.Re^{m}.Pr^{n}.(\frac{\mu}{\mu_0})^{0}$ Mechanical power: $(m.\dot{C}_p.\Delta t)_{oil} + Q_{H1/H2} + Q_{H2/H3}$ lumped model in matrix form: $K = \begin{matrix} I & O \\ (h.A)_{i/fluid} & K_{l/j} \end{matrix}$	Predicted TOT - <2% Predicted COT - <1%
2.	Serrano et al.	1-D lumped model	1. Water cooled and Non-water cooled turbocharger 2. Prediction of Pulsatile flow properties Using HTM.	Steady and Transient	1. Radial temperature Distribution is negligible 2. Heat transfer is followed by Work transfer	Conductive conductance: Fourier's law : $\dot{Q}_{ij}^{cond} = K_{ij}.(T_i - T_j)$ Convective conductance: Newton's law of cooling $\dot{Q}_{li}^{conv} = K_{li}.(T_i - T_j)$ Energy balance : $\left(K + hA + \frac{1}{\Delta t}C\right)T_i^{t+\Delta t} = Q + \frac{1}{\Delta t}C.T_i^{t} + hA.T_i^{t+\Delta t}$	1. Water- cooled turbocharger: Predicted TOT - ±10°C 2. Non-water-cooled turbocharger: Predicted TOT – almost zero deviation Predicted COT - ±5°C Importance of HTM is more noticeable in Non-water cooled turbocharger 3. Modeled enthalpy drop is less than measured enthalpy drop 4. Prediction of properties at pulsatile condition is better with HTM
		1-D lumped model	Influence of HT in full load Engine model – Turbine model – Compressor model	Steady	-	-	1. Hot map - HT/ML = Adiabatic map 2. Adiabatic map+HT/ML = Diabatic map 3. Better prediction of COT and TOT with HTM
		1-D lumped model	Advantage of HTM over LUM	Steady and Transient	Radial temperature distribution is negligible	Transient energy balance: $m_i c_i.\frac{dT_i}{dt} = c_i.\frac{dT_i}{dt} = \sum K_{ij}.(T_i - T_j)$	1. Predicted Speed: For LUM = <0.5% to 2% For HTM = ±1%. 2. Predicted TOT - improvement of 20-30K compared to LUM 3. Predicted COT - same accuracy for HTM and LUM
		1-D HT model	General correlation of HT modeling	Steady	Radial temperature distribution is negligible	Capacitance : Turbine: $C_T = \alpha.m_T.c_T$ Compressor : $C_c = \varepsilon.m_c.c_c$ Forced convection: $Nu = a.Pr^{b}.Re^{c}$ Radiation between nodes : $q_r = \frac{\sigma.(T_i^4 - T_j^4)}{\frac{1-\varepsilon_i}{A_i.\varepsilon_i} + \frac{1}{A_i.F_{i\to j}} + \frac{1-\varepsilon_j}{A_j.\varepsilon_j}}$	1.Predicted COT - ±5°C 2. Predicted TOT - improvement of over 15°C

Table 3- Summary of 1-D heat transfer modelling to date, from Romagnoli et al.[80] *(Page 2 of 3)*

3.	Westin et al.	1-D lumped model	Study of heat loss from turbine. Engine model – Turbine model	Steady	1. No radiation from Bearing housing	Radiation : Stafan – Boltzman's law – $\dot{Q}_{rad} = \epsilon.\sigma.A_{turb,surf}.T^4_{turb,surf}$ Conduction : Fourier's law: $\dot{Q} = K_{cond}.\Delta T$ Convection: Newton's law of cooling: $\dot{Q} = a.\Delta T$ Heat transport between components : $a.\Delta T_{env} + K_{cond/b}.\Delta T_b + K_{cond/m}.\Delta T_m = c.m_{turb}\left(\frac{dT}{dt}\right)_{turb}$	1. Without HTM, when heat loss is not considered -TOT prediction is > 50K compared to HTM. 2. Heat loss necessary to predict TOT is 35%, 28%, 8% at 1600 rpm, 1800 rpm and 1900 rpm respectively
4.	Cormerais et al	1-D HT model	Heat transfer under steady and transient analysis	Steady and Transient	Modeled as combination of Volumes and nozzles.	Forced convection: Nusselt number: $Nu = 0.023.Pr^{0.3}.Re^{0.8}$ Free convection: Nusselt number: $Nu = 0.53.(\mathrm{Gr.Pr})^{0.25}$ Heat transfer is calculated from energy balance : $\frac{dT}{dt} = \frac{h_{int}S_{cint}(T_f - T) + h_{ext}S_{cext}(T_0 - T) + \epsilon\sigma(T_0^4 - T^4)}{M.C}$	1. Transient exit temperature 2. Flow map 3. Turbine power and HT
5.	Burke et al.	1-D HT model	Study of heat addition before compression	Steady	1. Conduction within the Housing is negligible 2. Heat is added only before and after compression.	Total Convective heat transfer : $Q_{Total} = Q_b + Q_a = h_b h_b(T_1 - T_c) + h_a A_a(T_{2'} - T_c)$ Convection: Sieder-Tate: $(h.A)_{l/i} = a.Re_d^{a_2}.Pr^{a_3}.(\frac{\mu_{bulk}}{\mu_{skin}})^{a_4}$ Compressor exposed area: Internal area: $A_T = A_b + A_a = \alpha_A A_T + (1 - \alpha_A)A_T$	1. When exposed area $\propto_A$=0, compressor efficiency is overestimated. For, $\propto_A$ >0, compressor efficiency is underestimated 2. Prediction of apparent efficiency and COT Recommendation: Division of thermal node of compressor into two - compressor front face and rest of compressor.
		1-D lumped model	On-engine HT analysis	Steady and transient	1. Radial temperature distribution is negligible 2. Turbine side –Heat transfer occurs only before expansion 3. Compressor side- Heat transfer occurs only after compression	Conductive conductance: Fourier's law : $\dot{Q}_{ij}^{cond} = K_{ij}.(T_i - T_j)$ Convective conductance: Newton's law of cooling : $\dot{Q}_{li}^{conv} = K_{li}.(T_i - T_j)$	1. Predicted TOT - Steady state: improvement from 29°C to 13°C Transient state: improvement from 35°C to 14°C 2. Predicted Metal temperature: Compressor housing - within 17°C Turbine housing - within 15°C
		1-D HT model	HT between exhaust gas and turbine node	Steady, pulsating and transient	1. Work and heat transfer occurs independently 2. Heat transfer occurs is only before and after compression / expansion 3. Diffuser – constant diameter pipe, Tongue – constant diameter short pipe, Turbine -Two pipes of constant diameter	Energy balance: $m_T C_{p,T}\frac{dT_T}{dt} = Q_{b,T} + Q_{a,T} - Q_{T/B} - Q_{T.rad} - Q_{T,conv}$ Convection: Sieder-Tate: $Nu = c_1.Re_t^{c_2}.Pr^{1/3}.(\frac{\mu_{bulk}}{\mu_{skin}})^{0.14}$	Transient: Predicted TOT - improvement from 33°C to -3°C

Table 3- Summary of 1-D heat transfer modelling to date, from Romagnoli et al.[80] *(Page 3 of 3)*

6.	Baines et al.	HT network model	Heat transfer analysis	Steady	1. Constant ambient temperature 2. In internal heat transfer, radiation is neglected.	External heat transfer $Q_{ext} = Q_{conv} + Q_{rad} + Q_{cond}$ $= \bar{h}_s A_s (T_s - T_a) + \kappa A_c (T_s - T_a)/x + \epsilon\sigma (T_s^4 - T_a^4)$ Surface temperature: Forced convection: $Nu = a.Pr^b.Re^c$ Free convection : $Nu = d.Pr^f.Gr^e$ Conservation of energy: $m_{oil}(h_{0oil,out} - h_{0oil,in})=$ $P_T - P_C + Q_{T,int} - Q_{C,int} - Q_{Bext}$	Prediction of compressor and turbine external and internal heat transfer with good accuracy
7.	Romagnoli and Martinez-Botas	1-D lumped model	On-engine HT analysis	Steady	1. Heat is added only before and after compression. 2. Uniform wall thickness 3. Compressor, Turbine and Bearing housing are modeled as simple cylinder.	Conduction : Fourier's law $\dot{Q}_{cond} = -KA\frac{dT}{dx}$ Forced Convection: Newton's law of cooling: $\dot{Q}_{conv} = hA\Delta T$ Radiation: $\dot{Q}_{rad} = -\sigma A(T_{surf}^4 - T_{amb}^4)$ Heat transfer co-efficient: Turbine casing: Annular surface: $h_{t,surf1} = 0.667\frac{K_T}{D_T}Ra^{0.25}$ Cylinder ends: $h_{t,surf1} = 0.530\frac{K_T}{D_T}Ra^{0.25}$ Bearing housing: $h_{BP,surf} = 0.667\frac{K_{BP}}{D_{BP}}[Ra(y)]^{0.25}$ Turbine and Compressor : $h_{T,C} = 0.046\frac{2K}{D}Re^{0.8}Pr^{0.4}$	1. Predicted COT - maximum deviation is 5K 2. Predicted Diabatic efficiency η_{dia} −<3% 3. 3. Predicted Heat conducted - ΔQ average deviation - ±8%

Multi-Dimensional Heat Transfer Modelling

Experiments into heat transfer in turbochargers are often limited by the complexity of collecting detailed data of flow properties and temperature data throughout the device, since geometry can be complex and difficult to access with measuring devices. Since it's regularly not possible to obtain a complete picture of boundary conditions required for computational modelling, heat transfer simulation of the entire turbocharging system is not currently used in industry [80]. In order to perform a three-dimensional analysis of a turbocharger, researchers have adopted a method known as the Conjugate Heat Transfer method (CHT). By treating the fluid domains and solid domains separately and conjugating the solution, only a minimal amount of inputs are required, and these are usually obtained via experiment. The results obtainable via this method can be detailed and useful to designers. An example is given in Figure 28, where Burke et al. [68] used 3-D CHT modelling to plot absolute temperature (right of Figure 27) and temperature along the points on the line of a single flow-path through the compressor (illustrated on the left of Figure 27). Cases 1 and 2 are modelled with an insulated outer casing, with case 2 having an adiabatic condition set on the inner inducer and shroud walls, preventing heat transfer prior to compression. Case 3 was similar to case 1, but with the inclusion of external convection to ambient air.

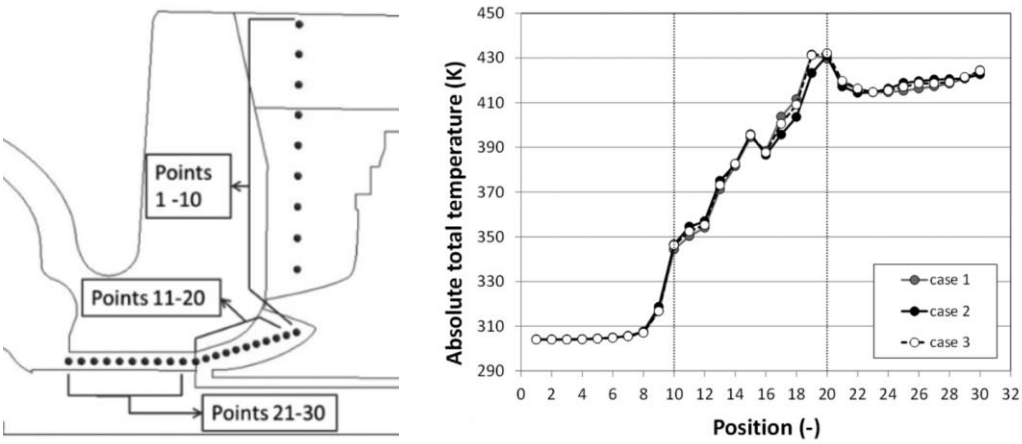

Figure 27 – A single flow path through a compressor (left) and the resulting temperature at points along that line, obtained via 3-D CHT simulation

In order to find a solution, the same numerical scheme and discretization method for both the fluid and solid zones, which are directly coupled. Calculation of external heat transfer can be avoided by using thermal imaging techniques [105] in combination with conventional inlet and outlet conditions. A study by Bohn et al. [105], [106] conducted CHT modelling and adopted thermal imaging software, also taking physical temperature measurements to verify accuracy. The authors also used their results to produce a set of emissivity constants used to account for radiation effects (commonly not accounted for by CHT models).

CHT is computationally expensive and time consuming in comparison with one-dimensional techniques, although this time can be reduced if used along with a one-dimensional

model [107]. Despite the additional complexity and computational time requirements, increasingly researchers are adopting CHT to study turbochargers and their individual components, such as the turbine, compressor or bearing housing. [68], [108], [109] The most commonly used turbulence models are the shear stress transport model for both the boundary layer [110] and the free stream [111], and the more efficient Baldwin-Lomax eddy viscosity model [80], [106], [112]. Although some have used the finite element method (FEM) to analyse heat transfer in three-dimensions [113], FEM is more often used in conjunction with the temperature fields found using CHT, in order to find the thermal stresses located in components that are subject to thermal loads [114].

In 2003, Bohn et al. [105], [106] used CHT methods to conclude that, when Reynold's number is low, compressor-side fluid is heated by transferred heat from the turbine side. At the high Reynold's numbers the heating effects caused by compression are significant enough to increase the temperature of the blades and casing; authors concluded that heat transfer from turbine to compressor significantly impacts the compression. Bohn et al.'s later investigation [115], gave details of the modelling method used (Figure 28) detailing the millions of cells required for simulation. The results of the simulation were provided in the form of temperature distributions for the compressor, bearing housing and turbine (right of Figure 28 for the compressor side). The authors found that the compressor fluid is heated up by heat flux from the turbine at low Reynold's numbers. At high Reynold's numbers the compression heating effect is significant enough to discharge heat into the casing and through the blades. This model was not compared with experimental data for verification, although the boundary conditions were input from previous experimental data collected by Bohn et al. [105].

In another study, Hellstrom et al. [116] used large eddy simulation (LES) to simulate a turbocharger in 3-D. They noted that the vortex structures that formed inside the turbine flow passages aided cooling by mixing cooler fluid, from the thermal boundary layer close to the walls, with the hot gases.

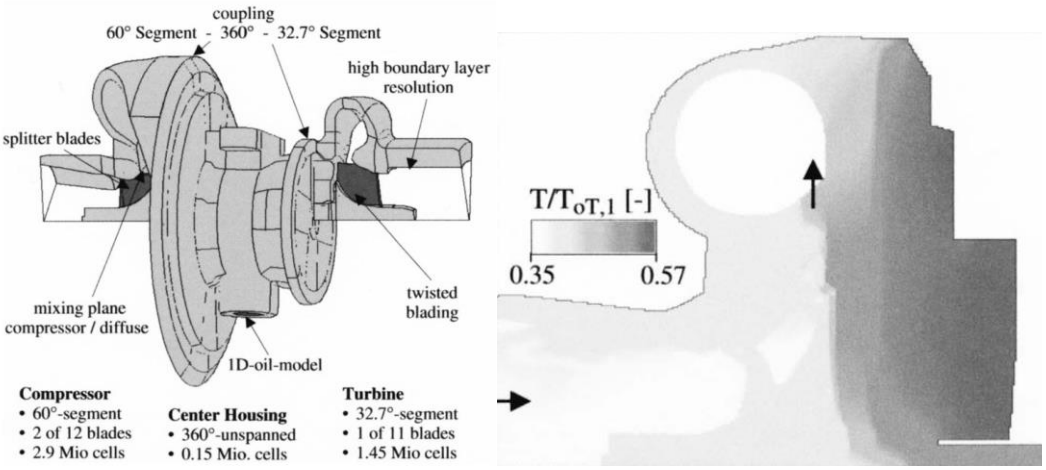

Figure 29- Geometrical model (left) and detailed non-dimensional temperature distribution results (right) of the CHT model developed by Bohn et al.[115]

CONCLUSION

This chapter has covered key principles of both heat transfer and unsteady flow phenomena in automotive turbomachinery, whilst also summarising the findings of theoretical and experimental research in both fields. To date, limited analysis has been done with a view of investigating heat transfer and pulsating flow effects in combination [80], this is largely down to the challenging experimental environment in which no simple solution has been found to measure all relevant parameters. Such experimental work requires high sensitivity sensors in a demandingly hot flow environment; other issues include limited space, and difficult accessibility for the location of all relevant instrumentation. Computational studies are demanding; due to their complexity, long calculation times and high software and hardware requirements are limiting factors.

In order to attain a complete picture of turbocharger performance at the design stage, performance maps (or their possible future replacement) must account for the effects of pulsating flows, heat transfer phenomena, and ideally be formed of a wider range of test data than is currently used in order to minimise the need for extrapolation techniques that add additional uncertainty and error into predictions. Instead of the current industrial test method, a pulsating flow rig such as those described in this chapter, would be capable of obtaining a wider range of performance data, minimising extrapolation. Heat transfer then needs to be accounted for either theoretically with modelling, or in a future scenario, with a test rig and methodology that is capable of quantifying all relevant variables in hot pulsating gas flows. Computational studies will become increasingly feasible in the future as compuatational power increases and becomes more affordable. At this stage, experimental testing could be limited to that required for the validation and calibration of complex computational models.

NOMENCLATURE

Abbreviation	**Descritpion**
CFD	Computational fluid dynamics
CHT	Conjugate heat transfer
ICE	Internal combustion engine
MFP	Mass flow parameter
PR	Pressure ratio
TIT	Turbine inlet temperature
VGT	Variable geometry turbocharger

Roman	**Description**
A	Area
Ar	Archimedes number
C	Velocity
Cp	Specific heat at constant pressure
g	Acceleration due to gravity
Gr	Grashof number

h	Specific enthalpy
K	Fraction of heat transfer
L	Length/Length scale
M	Mach number
ṁ	Mass flow rate
N	Rotational speed
Nu	Nusselt number
P	Pressure
Pr	Prandtl number
Q	Heat Transfer
R	Gas constant
R/r	Radius
Re	Reynold's number
S	Entropy
St	Strouhal number
T	Temperature
t	time
U	Blade speed
u	Compressor peripheral speed
V	Velocity
W	Work
x	Length

Greek	**Description**
β	Blade angle, in degrees
γ	Ratio of specific heats
ε	Emissivity
η	Efficiency
θ	Convective heat trasnfer coefficient
Θ	Temperature difference between fluid and surface
κ	Thermal conductivity
μ	Dynamic viscocity
ξ	Heat number
ρ	Density
σ	Stefan-Boltzmann constant
ς	Flow coefficient
τ	Time scale
φ	Phase difference/Azimuth Angle
X	Coefficient of volume expansion
ω	Angular velocity
Ω	Rotor angular speed

Subscript	Description
1	Compressor inlet
2	Compressor outlet
3	Turbine inlet
4	Turbine outlet
1*	Impeller inlet
2*	Impeller outlet
3*	Rotor inlet
4*	Rotor outlet
a	Ambient
adi	Adiabatic
after	after compression/expansion
before	before compression/expansion
c	Cross section
C	Comprssor
cond	Conduction
conv	Convection
dia	Diabatic
e	External surface
ex	Exit
ext	External
F/f	Fluid
in	Inlet
int	Internal
isen	Isentropic
m	Mean
mech	Mechanical
mer	Meridonal component
out	Outlet
P/p	Pulse/Pressure/Peripheral
r	Revolution
rad	Radiation
s	Surface
T	Temperature/Turbine
tot	Total condition
t-s	Total-to-static

REFERENCES

[1] A. Pesiridis, S. Lioutas, and R. F. Martinez-Botas, "Integration of Unsteady Effects in the Turbocharger Design Process," *Proc. ASME Turbo Expo 2012*, pp. 1–13, 2012.

[2] M. S. Chiong, S. Rajoo, A. Romagnoli, A. W. Costall, and R. F. Martinez-Botas, "Integration of meanline and one-dimensional methods for prediction of pulsating performance of a turbocharger turbine," *Energy Convers. Manag.*, vol. 81, pp. 270–281, 2014.

[3] M. Gugau and H. Roclawski, "On the Design and Matching of Turbocharger Turbines," in *Proceedings of ASME Turbo Expo 2012. Paper No. GT2012-68575*, 2012, pp. 1–10.

[4] I. Hakeem, C.-C. Su, A. W. Costall, and R. F. Martinez-Botas, "Effect of volute geometry on the steady and unsteady performance of mixed-flow turbines," *Proc. Inst. Mech. Eng. Part A J. Power Energy*, vol. 221, no. 4, pp. 535–549, 2007.

[5] E. Greitzer, "An Introduction to Unsteady Flow in Turbomachines," *Thermodyn. Fluid Mech. Turbomach.*, vol. II of NATO, no. E: Applied Sciences, pp. 967–1025, 1985.

[6] H. Chen and D. E. Winterbone, "A one-dimensional performance model for turbocharger turbine under pulsating inlet condition," in *11th International Conference on Turbochargers and Turbocharging*, 2014, pp. 113–123.

[7] A. Dale, "Radial, vaneless, turbocharger turbine performance," Imperial College of Science, Technology and Medicine, University of London, UK, 1990.

[8] F. J. Wallace and G. P. Blair, "Pulsating-flow performance of inward radial-flow turbines," *Proc ASME Meet. GTP21 Feb 28Mar 4 1965*, p. 20, 1965.

[9] R. S. Benson and K. H. Scrimshaw, "An experimental investigation of non-steady flow in a radial gas turbine," *Proc. Inst. Mech. Eng. Conf. Proc.*, vol. 180 Part 3, no. 10, pp. 74–85, 1965.

[10] F. J. Wallace, P. R. Cave, and J. Miles, "Performance of Inward Radial Flow Turbines Under Steady Flow Conditions with Special Reference to High Pressure Ratios and Partial Admission," in *Proc Instn Mech Engrs 1969-70*, 1970, pp. 1027–1042.

[11] F. J. Wallace and J. Miles, "Performance of Inward Radial Flow Turbines Under Unsteady Flow Conditions with Full and Partial Admission," in *Proc lnstn Mech Engrs 1970-71*, 1970, vol. 185, no. 77/71, pp. 1091–1105.

[12] T. Miyashita, T. Tomita, and D. Ishihara, "Performance of inward radial flow turbines under unsteady flow conditions," *IHI Eng. Rev.*, vol. 7, no. 1, 1974.

[13] R. S. Benson, "Non steady flow in a turbocharger nozzleless radial gas Turbine.," *Trans. SAE*, vol. Paper No., 1974.

[14] H. Kosuge, N. Yamanaka, I. Ariga, and I. Watanbe, "Performance of radial flow turbines under pulsating flow conditions," *Trans. ASME*, vol. 98, pp. 53–59, 1976.

[15] M. Capobianco, A. Gambarotta, and G. Cipolla, "Influence of the pulsating flow operation on the turbine characteristics of a small internal combustion engine turbocharger.," in *Proc. Instn. Mech. Engr. Paper No. C372/019*, 1989.

[16] M. Capobianco and A. Gambarotta, "Unsteady flow performance of turbocharger radial turbines," in *4th Int. Conf. on Turbocharging and Turbochargers, Inst. Mech. Engr. Paper No. C405/017*, 1990.

[17] M. Capobianco and A. Gambarotta, "Variable geometry and waste-gated automotive turbocharges: Measurements and comparison of turbine performance," *J. Eng. Gas Turbines Power*, vol. 114, pp. 553–560, 1992.

[18] N. C. Baines, "Turbocharger turbine pulse flow performance and modelling – 25 years on," *Proc IMechE Turbochargers Turbocharging Congr. 2010*, no. 7, pp. 347–362, 2010.

[19] A. Dale and N. Watson, "Vaneless Radial Turbocharger Turbine Performance," in *Proceedings of the Institution of Mechanical Engineers, 3rd International Conference on*

Turbocharging and Turbochargers, 1986.

[20] J. H. Yeo and N. C. Baines, "Pulsating flow behaviour in a twin-entry vaneless radial-inflow turbine.," in *IMechE Conference on Turbochargers and Turbocharging*, 1990, pp. 113–122.

[21] N. C. Baines and J. H. Yeo, "Flow in a radial turbine under equal and partial admission conditions," in *Turbomachinery: Latest Developments in a Changing Scene*, 1991, pp. 103–112.

[22] N. C. Baines, A. Hajilouy-Benisi, and J. H. Yeo, "The pulse flow performance and modelling of radial inflow turbines," in *Proc. IMechE. Conf. Turbochargers and Turbocharging*, 1994, pp. 209–220.

[23] H. Chen and D. E. Winterbone, "A method to predict performance of vaneless radial turbines under steady and unsteady flow conditions," *IMechE J. Turbochargers Turbocharging*, pp. 13–22, 1990.

[24] D. E. Winterbone, B. Nikpour, and G. I. Alexander, "Measurement of the performance of a radial inflow turbine in conditional steady and unsteady flow," in *Proceedings of the Institution of Mechanical Engineers fourth international conference turbocharging and turbochargers 1990-6*, 1990, pp. 153–162.

[25] D. E. Winterbone, B. Nikpour, and H. Frost, "A Contribution to the Understanding of Turbocharger Turbine Performance in Pulsating Flow," in *Internal combustion engine research in universities, polytechnics and colleges, conference*, 1991, pp. 19–29.

[26] A. Romagnoli, R. F. Martinez-Botas, and S. Rajoo, "Turbine performance studies for automotive turbochargers. Part 2: Unsteady analysis," *9th Int. Conf. Turbochargers Turbocharging - Inst. Mech. Eng. Combust. Engines Fuels Gr.*, pp. 387–408, 2010.

[27] A. Romagnoli, S. Rajoo, and R. F. Martinez-Botas, "Turbine Performance Studies for Automotive Turbochargers Part One: Steady Analysis," in *9th International Conference on Turbochargers and Turbocharging - Institution of Mechanical Engineers, Combustion Engines and Fuels Group*, 2009.

[28] N. Karamanis and R. F. Martinez-Botas, "Mixed-flow turbines for automotive turbochargers: steady and unsteady performance," *Int. J. Engine Res.*, vol. 3, no. 3, pp. 127–138, 2002.

[29] S. Szymko, R. F. Martinez-Botas, and K. R. Pullen, "Experimental Evaluation of Turbocharger Turbine Performance Under Pulsating Flow Conditions," in *Volume 6: Turbo Expo 2005, Parts A and B*, 2005, pp. 1447–1457.

[30] A. Pesiridis and R. F. Martinez-Botas, "Experimental Evaluation of Active Flow Control Mixed-Flow Turbine for Automotive Turbocharger Application," *ASME Conf. Proc.*, vol. 127, pp. 44–52, 2007.

[31] C. D. Copeland, R. Martinez-Botas, and M. Seiler, "Unsteady Performance of a Double Entry Turbocharger Turbine With a Comparison to Steady Flow Conditions," *ASME Conf. Proc.*, vol. 2008, no. 43161, pp. 1579–1588, 2008.

[32] A. W. Costall, "A one-dimensional study of unsteady wave propagation in turbocharger turbines," Imperial College London, 2008.

[33] A. W. Costall, R. M. McDavid, R. F. Martinez-Botas, and N. C. Baines, "Pulse Performance Modeling of a Twin Entry Turbocharger Turbine Under Full and Unequal Admission," in *Proceedings of ASME Turbo Expo 2009: Power for Land, Sea and Air*, 2009, no. GT2009-59406.

[34] S. Szymko, "The Development of an Eddy Current Dynamometer for Evaluation of Steady and Pulsating Turbocharger Turbine Performance," Imperial College London, 2006.

[35] M. Yang and R. F. Martinez-Botas, "Influence of Volute Cross-Sectional Shape of a Nozzleless Turbocharger Turbine Under Pulsating Flow Conditions," *Proc. ASME Turbo Expo 2014 Turbine Tech. Conf. Expo.*, no. GT2014-26150, pp. 1–11, 2014.

[36] J. R. Serrano, F. J. Arnau, P. Fajardo, M. a. Reyes Belmonte, and F. Vidal, "Contribution to the Modeling and Understanding of Cold Pulsating Flow Influence in the Efficiency of Small Radial Turbines for Turbochargers," *J. Eng. Gas Turbines Power*, vol. 134, no. October, p. 102701, 2012.

[37] F. Payri, J. Galindo, J. R. Serrano, and M. Reyes-Belmonte, "Experimental methodology to a Comprehensive Characterization of Automotive Turbochargers," in *EAEC 2011*, 2011.

[38] A. J. Feneley, A. Pesiridis, and A. M. Andwari, "Variable Geometry Turbocharger Technologies for Exhaust Energy Recovery and Boosting- A Review," *Renew. Sustain. Energy Rev.*, vol. 71, no. December 2016, pp. 959–975, 2016.

[39] M. Capobianco and S. Marelli, "Experimental investigation into the pulsating flow performance of a turbocharger turbine in the closed and open waste-gate region," *9th Int. Conf. Turbochargers Turbocharging - Inst. Mech. Eng. Combust. Engines Fuels Gr.*, pp. 373–385, 2010.

[40] M. Capobianco and S. Marelli, "Experimental analysis of unsteady flow performance in an automotive turbocharger turbine fitted with a waste-gate valve," *Proc. Inst. Mech. Eng. Part D J. Automob. Eng.*, vol. 225, no. 8, pp. 1087–1097, 2011.

[41] M. Capobianco and S. Marelli, "Turbocharger Turbine Performance Under Steady and Unsteady Flow: Test Bed Analysis and Correlation Criteria," in *Proc. 8th International Conference on Turbochargers and Turbocharging*, 2006.

[42] M. Capobianco and S. Marelli, "Waste-Gate Turbocharging Control in Automotive SI Engines : Effect on Steady and Unsteady Turbine Performance," *SAE Pap. 2007-01-3543*, pp. 776–790, 2007.

[43] F. Bozza, V. De Bellis, S. Marelli, and M. Capobianco, "1D Simulation and Experimental Analysis of a Turbocharger Compressor for Automotive Engines under Unsteady Flow Conditions," *SAE Int. J. Engines*, vol. 4, no. 1, pp. 1365–1384, 2011.

[44] V. De Bellis, S. Marelli, F. Bozza, and M. Capobianco, "1D simulation and experimental analysis of a turbocharger turbine for automotive engines under steady and unsteady flow conditions," *Energy Procedia*, vol. 45, pp. 909–918, 2014.

[45] S. Marelli and M. Capobianco, "Steady and pulsating flow efficiency of a waste-gated turbocharger radial flow turbine for automotive application," *Energy*, vol. 36, no. 1, pp. 459–465, 2011.

[46] H. Pucher, "Overall Engine Process Simulation - an important tool for the development of supercharged engines," *IMechE J. Turbochargers Turbocharging*, pp. 155–166, 2002.

[47] D. E. Winterbone and R. J. Pearson, *Design Techniques for Engine Manifolds: Wave Action Methods for IC Engines*. Wiley, 1999.

[48] D. E. Winterbone, R. J. Pearson, and J. Horlock, *Theory of Engine Manifold Design: Wave Action Methods for IC Engines*. Wiley, 2000.

[49] X. Hu and P. B. Lawless, "A model for radial flow turbomachine performance in highly unsteady flows," *ASME Pap. 2001-GT-0312*, 2001.

[50] H. Chen, I. Hakeem, and R. F. Martinez-Botas, "Modelling of a turbocharger turbine under pulsating inlet conditions," *Proc. Inst. Mech. Eng. Part A J. Power Energy*, vol. 210, no. 5, pp. 397–408, 1996.

[51] M. Abidat, M. Hachemi, M. K. Hamidou, and N. C. Aines, "Prediction of the steady and non-steady flow performance of a highly loaded mixed flow turbine," in *Proc Instn Mech Engrs*, 1998, vol. 212 Part A, no. May 1998, pp. 173–184.

[52] A. W. Costall, S. Szymko, R. F. Martinez-Botas, D. Filsinger, and D. Ninkovic, "Assessment of Unsteady Behavior in Turbocharger Turbines," in *ASME. Turbo Expo: Power for Land, Sea, and Air, Volume 6: Turbomachinery, Parts A and B*, 2006, pp. 1023–1038.

[53] D. Ehrlich, "Characterization of unsteady on-engine turbocharger turbine boundary conditions," Purdue University, 1998.

[54] D. Ehrlich, P. B. Lawless, and S. Fleeter, "On-Engine Turbocharger Turbine Inlet Flow Characterization," *SAE Pap.*, no. 412, p. 971565, 1997.

[55] X. Hu and P. B. Lawless, "Predictions of On-Engine Efficiency for The Radial Turbine of a Pulse Turbocharged Engine," *Sae*, vol. SAE 2001 W, no. 724, p. 10, 2001.

[56] X. Hu, "Experimental Evaluation of Turbocharger Turbine Performance Under Pulsating Flow Conditions," Purdue University, 2000.

[57] A. J. King, "A turbocharger unsteady performance model for the GT-Power internal combustion engine simulation," *ProQuest Diss. Theses*, p. 148-148 , 2002.

[58] A. J. Feneley, A. Pesiridis, and H. Chen, "A One-Dimensional Gas Dynamics Code for Turbocharger Turbine Pulsating Flow Performance Modelling," in *Proceedings of ASME Turbo Expo 2017: Gas Turbine Technical Conference and Exposition. Paper No. GT2017-64743*, 2017.

[59] J. K.-W. Lam, Q. D. H. Roberts, and G. T. McDonnell, "Flow modelling of a turbocharger turbine under pulsating flow," in *Turbochargers and turbocharging, 7th International conference*, 2002, pp. 181–197.

[60] D. Palfreyman and R. F. Martinez-Botas, "The Pulsating Flow Field in a Mixed Flow Turbocharger Turbine: An Experimental and Computational Study," *ASME Conf. Proc.*, vol. 2004, no. 41707, pp. 697–708, 2004.

[61] F. Hellstrom and L. Fuchs, "Numerical Computation of the Pulsatile Flow in a Turbocharger," *Proc. ASME*, 2009.

[62] F. Hellstrom and L. Fuchs, "Effects of Inlet Conditions on the Turbine Performance of a Radial Turbine," *ASME Conf. Proc.*, vol. 2008, no. 43161, pp. 1985–2001, 2008.

[63] F. Hellström, "Numerical computations of the unsteady flow in a radial turbine," KTH Stockholm, 2010.

[64] N. K. and D. P. and C. A. and R. F. Martinez-Botas, "Steady and Unsteady Velocity Measurements in a Small Turbocharger Turbine with Computational Validation," *J. Phys. Conf. Ser.*, vol. 45, no. 1, p. 173, 2006.

[65] P. Chesse, D. Chalet, and X. Tauzia, "Impact of the Heat Transfer on the Performance Calculations of Automotive Turbocharger Compressor R&D for Cleaner and Fuel Efficient Engines and Vehicles R&D pour des véhicules et moteurs plus propres et économes," *Oil Gas Sci. Technol. – Rev. IFP Energies Nouv.*, vol. 66, no. 5, pp. 791–800, 2011.

[66] M. Cormerais, J. F. Hetet, P. Chesse, and A. Maiboom, "Heat Transfer Analysis in a Turbocharger Compressor : Modeling and Experiments," *SAE Tech. Pap. Ser. Pap. No. 2006-01-0023*, 2006.

[67] N. C. Baines, K. Wygant, and A. Dris, "The Analysis of Heat Transfer in Automotive Turbochargers," in *Proceedings of ASME Turbo Expo 2009: Power for Land, Sea and Air*, 2009.

[68] R. D. Burke, C. D. Copeland, T. Duda, and M. A. Rayes-Belmote, "Lumped Capacitance and Three-Dimensional Computational Fluid Dynamics Conjugate Heat Transfer Modeling of an Automotive Turbocharger," *J. Eng. Gas Turbines Power*, vol. 138, no. 9, p. 92602, 2016.

[69] B. Sirakov and M. Casey, "Evaluation of Heat Transfer Effects on Turbocharger Performance," *J. Turbomach.*, vol. 135, no. March, p. 21012, 2013.

[70] M. V. Casey and T. M. Fesich, "The Efficiency of Turbocharger Compressors With Diabatic Flows," *J. Eng. Gas Turbines Power*, vol. 132, no. July, p. 72302, 2010.

[71] M. V. Casey and M. Schlegel, "Estimation of the performance of turbocharger compressors at extremely low pressure ratios," *Proc. Inst. Mech. Eng. Part A J. Power Energy*, vol. 224, no. 2, pp. 239–250, 2010.

[72] A. Romagnoli, "Aerodynamic and thermal characterization of turbocharger turbines: experimental and computational evaluation," Imperial College London, 2010.

[73] D. Hagelstein, B. Beyer, J. Seume, M. Rautenberg, and H. Hasemann, "Heuristical view on the non-adiabatic coupling system of combustion engine and turbocharger," in *IMechE 7th International Conference on Turbochargers and Turbocharging*, 2002.

[74] S. Shaaban and J. R. Seume, "Analysis of Turbocharger Non-Adiabatic Performance," *8th Int. Conf. Turbochargers Turbocharging*, pp. 119–130, 2006.

[75] M. Rautenberg, M. Malobabic, and A. Mobarak, "Influence of heat transfer between turbine and compressor on the performance of small turbochargers," in *Tokyo International Gas Turbine Congress*, 1983, pp. 567–574.

[76] M. Rautenberg and N. Kammer, "On the Thermodynamics of Non-Adiabatic Compression

and Expansion Process in Turbomachines," in *ICMPE, Proceedings of the 5th International Conference for Mechanical Power Engineering*, 1984.

[77] M. Malobabic and M. Rautenberg, "Adiabatic and non-adiabatic efficiencies of small turbochargers," in *GTSJ International Gas Turbine Congress. Paper No. IGTC-105*, 1987, pp. 157–164.

[78] H. Aghaali, "On-Engine Turbocharger Performance Considering Heat Transfer," Royal Institute of Technology (KTH), Sweden, 2012.

[79] Pollux-EMS, "Hot Gas Test Benches," 2017. [Online]. Available: http://www.pollux-ems.com/english/testing-facilities-services/hot-gas-test-benches/index.html. [Accessed: 21-Apr-2017].

[80] A. Romagnoli *et al.*, "A Review of Heat Transfer in Turbochargers," *Renew. Sustain. Energy Rev. (IN Press.*, 2017.

[81] S. Shaaban and J. Seume, "Impact of turbocharger non-adiabatic operation on engine volumetric efficiency and turbo lag," *Int. J. Rotating Mach.*, vol. 2012, 2012.

[82] R. Burke, P. Olmeda, and J. R. Serrano, "Dynamic Identification of Thermodynamic Parameters for Turbocharger Compressor Models," in *Proceedings of the ASME 2014 Internal Combustion Engine Division Fall Technical Conference, Paper No. ICEF2014-5562*, 2014.

[83] J. R. Serrano, P. Olmeda, F. J. Arnau, A. Dombrovsky, and L. Smith, "Turbocharger heat transfer and mechanical losses influence in predicting engines performance by using one-dimensional simulation codes," *Energy*, vol. 86, pp. 204–218, 2015.

[84] A. Romagnoli and R. Martinez-Botas, "Heat transfer on a turbocharger under constant load points," *Proc. ASME Turbo Expo*, vol. 5, pp. 163–174, 2009.

[85] R. D. Burke, "Analysis and Modelling of the Transient Thermal Behaviour of Automotive Turbochargers," *J. Eng. Gas Turbines Power*, vol. 136, no. October 2014, p. V002T06A012, 2014.

[86] R. Burke, C. R. M. Vagg, D. Chalet, and P. Chesse, "Heat transfer in turbocharger turbines under steady, pulsating and transient conditions," *Int. J. Heat Fluid Flow*, vol. 52, pp. 185–197, 2015.

[87] F. Payri, P. Olmeda, F. J. Arnau, A. Dombrovsky, and L. Smith, "External heat losses in small turbochargers: Model and experiments," *Energy*, vol. 71, pp. 534–546, 2014.

[88] D. Verstraete and C. Bowkett, "Impact of heat transfer on the performance of micro gas turbines," *Appl. Energy*, vol. 138, pp. 445–449, 2015.

[89] J. R. Serrano, P. Olmeda, A. Páez, and F. Vidal, "An experimental procedure to determine heat transfer properties of turbochargers," *Meas. Sci. Technol.*, vol. 21, no. 3, p. 35109, 2010.

[90] J. R. Serrano, F. J. Arnau, V. Dolz, A. Tiseira, and C. Cervelló, "A model of turbocharger radial turbines appropriate to be used in zero- and one-dimensional gas dynamics codes for internal combustion engines modelling," *Energy Convers. Manag.*, vol. 49, no. 12, pp. 3729–3745, 2008.

[91] R. D. Burke, P. Olmeda, F. Arnau, and M. Rayes-Belmonte, "Modelling of Turbocharger heat transfer under stationary and transient conditions," in *11th International Conference on Turbochargers and Turbocharging*, 2014.

[92] J. R. Serrano, V. Dolz, A. Tiseira, and A. Páez, "Influence of Environmental Conditions and Thermodynamic Considerations in the Calculation of Turbochargers Efficiency h Compressor process h Turbine process," *SAE Tech. Pap. Ser. Pap. No. 2009-01-1468*, 2009.

[93] M. Cormerais, J. F. Hetet, P. Chessé, and A. Maiboom, "Heat Transfers Characterisations in a Turbocharger: Experiments and Correlations," no. 42061. pp. 53–64, 2006.

[94] G. Tanda, S. Marelli, G. Marmorato, and M. Capobianco, "An experimental investigation of internal heat transfer in an automotive turbocharger compressor," *Appl. Energy*, vol. 193, pp. 531–539, 2017.

[95] M. Jung, R. G. Ford, K. Glover, N. Collings, U. Christen, and M. J. Watts, "Parameterization and Transient Validation of a Variable Geometry Turbocharger for Mean-Value Modeling

at Low and Medium Speed-Load Points," *Powertrain Fluid Syst.*, no. 724, 2002.
[96] J. R. Serrano, P. Olmeda, F. J. Arnau, A. Dombrovsky, and L. Smith, "Methodology to Characterize Heat Transfer Phenomena in Small Automotive Turbochargers: Experiments and Modelling Based Analysis," in *Volume 1B: Marine; Microturbines, Turbochargers and Small Turbomachines; Steam Turbines*, 2014, p. V01BT24A003.
[97] S. Marelli, G. Marmorato, and M. Capobianco, "Evaluation of heat transfer effects in small turbochargers by theoretical model and its experimental validation," *Energy*, vol. 112, pp. 264–272, Oct. 2016.
[98] S. Marelli, S. Gandolfi, and M. Capobianco, "Heat Transfer Effect on Performance Map of a Turbocharger Turbine for Automotive Application," in *SAE Technical Paper*, 2017.
[99] I. A. Mohd, "Heat Distribution Study in Turbocharger Turbine's Volute," Universiti Teknologi Malaysia, 2013.
[100] J. R. Serrano, C. Guardiola, V. Dolz, A. Tiseira, and C. Cervelló, "Experimental study of the turbine inlet gas temperature influence on turbocharger performance," *SAE Tech. Pap.*, no. 724, pp. 776–790, 2007.
[101] M. Cormerais, "Caractérisation expérimentale et modélisation des transferts thermiques au sein d'un turbocompresseur automobile : application à la simulation du comportement transitoire d'un moteur diesel à forte puissance spécifique (In French)," l'Université de Nantes et de l'Ecole Centrale de Nantes, 2007.
[102] M. A. Reyes Belmonte, "Contribution to the Experimental Characterization and 1-D Modelling of Turbochargers for IC Engines," Universitat Politècnica de València, Valencia (Spain), 2013.
[103] A. Romagnoli and R. F. Martinez-Botas, "Heat transfer analysis in a turbocharger turbine: An experimental and computational evaluation," *Appl. Therm. Eng.*, vol. 38, pp. 58–77, 2012.
[104] R. Burke, C. Copeland, and T. Duda, "Investigation into the Assumptions for Lumped Capacitance Modelling of Turbocharger Heat Transfer," *6th Int. Conf. Simul. Test.*, 2014.
[105] D. Bohn, N. Moritz, and M. Wolff, "Conjugate Flow and Heat Transfer Investigation of a Turbo Charger: Part II — Experimental Results," in *ASME Turbo Expo 2003, collocated with the 2003 International Joint Power Generation Conference*, 2003.
[106] D. Bohn, T. Heuer, and K. Kusterer, "Conjugate Flow and Heat Transfer Investigation of a Turbo Charger: Part I — Numerical Results," in *ASME Turbo Expo 2003, collocated with the 2003 International Joint Power Generation Conference*, 2003.
[107] V.-M. Lei and T. Kawakubo, "A Fast Method for Conjugate Heat Transfer Analysis of Centrifugal Compressor," in *Volume 8: Heat Transfer, Fluid Flows, and Thermal Systems, Parts A and B*, 2007, pp. 699–706.
[108] B. Hoepke, M. Vieweg, and S. Pischinger, "Numerical analysis of energy flow paths in exhaust gas turbochargers by means of conjugate heat transfer," *J. Eng. Gas Turbines Power*, vol. 139, no. c, 2016.
[109] L. San Andrés, V. Barbarie, A. Bhattacharya, and K. Gjika, "On the Effect of Thermal Energy Transport to the Performance of (Semi) Floating Ring Bearing Systems for Automotive Turbochargers," *J. Eng. Gas Turbines Power*, vol. 134, no. October 2012, p. 102507, 2012.
[110] T. Heuer, B. Engels, and P. Wollscheid, "Thermomechanical Analysis of a Turbocharger Based on Conjugate Heat Transfer," in *ASME Turbo Expo 2005: Power for Land, Sea, and Air*, 2005, no. 1, pp. 829–836.
[111] P. Olmeda, V. Dolz, F. J. Arnau, and M. A. Reyes-Belmonte, "Determination of heat flows inside turbochargers by means of a one dimensional lumped model," *Math. Comput. Model.*, vol. 57, no. 7–8, pp. 1847–1852, 2013.
[112] T. Heuer and B. Engels, "Numerical Analysis of the Heat Transfer in Radial Turbine Wheels of Turbo Chargers," in *ASME. Turbo Expo: Power for Land, Sea, and Air, Volume 3: Turbo Expo 2007*, 2007, pp. 959–968.
[113] R. M. Nguru, K. S. Chapman, and J. Shultz, "Simplified methodology to correct

turbocharger field measurements for heat transfer and other effects," 2002.

[114] X. Zheng, L. Jin, T. Du, B. Gan, F. Liu, and H. Qian, "Effect of temperature on the strength of a centrifugal compressor impeller for a turbocharger," *Proc. Inst. Mech. Eng. Part C J. Mech. Eng. Sci.*, vol. 227, no. 5, pp. 896–904, 2012.

[115] D. Bohn, T. Heuer, and K. Kusterer, "Conjugate Flow and Heat Transfer Investigation of a Turbo Charger," *J. Eng. Gas Turbines Power*, vol. 127, no. July 2005, p. 663, 2005.

[116] F. Hellström and L. Fuchs, "Assessment of Heat Transfer Effects on the Performance of a Radial Turbine using Large Eddy Simulation," *IMechE, 9th Conf. turbochargers turbocharging*, pp. 281–291, 2010.